ISSN: 2754-4915

Journal of Material Sciences & Manufacturing Research

SCIENTIFIC Research and Community

Research Article

Open Access

Sustainable Binder Strategies: Comparative Effects of Palm Oil Fuel Ash in High-Volume GGBS Concrete

Aron Teji[1], Ash Ahmed[2*], An Huynh[3], Colin Yates[4] and Lee Yates[4]

[1]Researcher

[2]Associate Professor

[3]Lecturer, Civil Engineering Group, School of Built Environment & Engineering, Leeds Beckett University, UK

[4]Conserv Lime Products, UK

ABSTRACT

Concrete faces persistent challenges to its durability, performance, and sustainability, including cracking from thermal and shrinkage stresses, chemical degradation, freeze-thaw damage, and the high carbon footprint of cement production; workability, curing, and maintenance further complicate its use.

This study evaluates the combined use of POFA and GGBS as partial cement replacements to improve sustainability and mechanical performance, identifies methodological gaps in typical POFA characterisation, and demonstrates that modest POFA additions in high-volume GGBS binders can reduce CO_2e while mitigating early-age strength limitations of latent hydraulic systems.

POFA was introduced at 0-6% replacement in 1% increments within an 80% GGBS binder matrix across four secondary binders: ordinary Portland cement, Portland-limestone cement, natural hydraulic lime, and calcium air-lime. Compressive and flexural strengths were measured at 7, 14, 28, and 91 days using a 1:1:2 aggregate mix and water binder ratio of 0.40; water submersion and ambient curing were compared at 28 and 91 days.

Incorporation of POFA in GGBS/CEM I composites yielded compressive strengths above C30/37 MPa, a 16.6% increase over the control, and improved workability. Optimal POFA contents for peak flexural strength were binder dependent: 2-3% for GGBS/CEM I, 5% for GGBS/CEM II and GGBS/CL90, and 6% for GGBS/NHL5, implicating filler effects, particle packing, latent hydraulicity, and secondary pozzolanic reactions in microstructural refinement. Mixes were highly curing-sensitive with strength variations up to 33% resulting in a compressive strength ranking CEM I > CEM II > CL90 > NHL5, while CEM II and NHL5 showed similar responses to POFA.

Significant compositional variability in both the chemistry and morphology of POFA was evident in the literature and this sample, underscoring the need for fraction-specific chemical and mineralogical characterisation. These results indicate that carefully optimised, low-level POFA additions to high-volume GGBS binders can enhance performance and reduce clinker demand, supporting more sustainable cementitious formulations.

***Corresponding author**

Ash Ahmed, Associate Professor, Civil Engineering Group, School of Built Environment & Engineering, Leeds Beckett University, UK.

Received: February 09, 2026; **Accepted:** February 16, 2026; **Published:** February 21, 2026

Keywords: Hydraulic Lime, Hydrated Lime, Ordinary Portland Cement, Portland-Limestone Cement, Concrete, Ground Granulated Blast Furnace Slag, Palm Oil Fuel Ash, Compressive Strength

Introduction and Background

The environmental impact of cement production, being 8-10% of anthropologic CO_2 emissions, has prompted widespread interest in supplementary cementitious materials (SCMs) that can reduce clinker content while maintaining or enhancing concrete performance [1-4]. Among these, Ground Granulated Blast Furnace Slag (GGBS) has been extensively studied and adopted due to its latent hydraulic properties and proven ability to improve durability and reduce embodied carbon (CO_2e) [5-13]. However, in regions where GGBS utilisation is already near saturation, further reductions in CO_2e require the integration of additional SCMs and more strategic binder combinations.

In the European CEM family of cement, CEMII, CEMIII, and CEMV all include GGBS in varying proportions, ranging from 6-20% for CEMII/A-S to a maximum of 81-95% for CEMIII/C [14]. Additionally, GGBS is utilised in the production of super sulphated cements (SSC), geopolymers, and alkali-activated materials (AAM) [15,16]. Blast furnace cement (CEMIII) replaces from 36% to 95% of the Ordinary Portland Cement (OPC) clinker with GGBS. CEMIII/B replaces 66-80% of the clinker with GGBS.

In this study, the GGBS replaced CEMI samples are thus analogous to a borderline CEMIII/B to CEMIII/C compositions, with 77-80% clinker replacement, and a midrange CEMIII/C composition with 87-90% clinker replacement, used as controls.

GGBS is already utilised at near full capacity in many regions, particularly within industrialised economies [17]. As such, its continued deployment should be strategically optimised to ensure it delivers meaningful reductions in CO_2e at a global scale. Rather than serving as a marginal offset for individual construction projects, GGBS should be integrated into broader decarbonisation frameworks that prioritise systemic impact.

To be truly effective as a CO_2e -reducing SCM, its use should be aligned with lifecycle-based design strategies, regional material availability, and long-term sustainability goals. This requires shifting from opportunistic substitution to deliberate, performance-driven applications that maximise its latent potential in reducing clinker content, enhancing durability, and extending service life.

This study contributes to that goal by comparing the performance of high-volume GGBS concrete when paired with four distinct secondary binder materials:

- OPC specifically (CEMI/52.5R),
- Portland-Limestone Cement (PLC) specifically (CEMII/A-L 32.5R),
- Natural Hydraulic Lime (NHL) specifically (NHL5), and
- Hydrated Calcium Air-Lime (CL) specifically (CL90).

Each binder presents unique hydration characteristics, strength development profiles, and environmental footprints, which influence the overall efficacy of GGBS as an SCM.

By evaluating these combinations under controlled conditions, the research identifies binder systems that not only enhance mechanical performance but also support scalable, low-carbon concrete design. This comparative approach enables a more deliberate and context-sensitive deployment of GGBS, moving beyond isolated project-level offsets toward integrated strategies for global decarbonisation in the construction sector.

To advance the strategic deployment of GGBS as a globally impactful SCM, this study incorporates Palm Oil Fuel Ash (POFA) into binary high-volume GGBS concrete and evaluates its performance across the four distinct secondary binder systems.

POFA, an agro-industrial by-product rich in silica, has emerged as a promising partial cement replacement (PCR) due to its pozzolanic reactivity and environmental benefits [18]. When used in binary systems with high-volume GGBS, POFA contributes to secondary hydration and pozzolanic reactions, enhancing long-term strength and reducing permeability. Studies have shown that POFAGGBS blends can improve workability and mechanical properties, particularly when used at moderate replacement levels (10-20%) [19, 20]. However, it generally has an adverse effect on workability with increasing dosage, without supplemental superplasticiser additions [21, 22]. When combined with plasticisers, the unburned carbon particulates have been found to influence dosage, i.e. with increasing unburned carbon increasing dosage requirements [23].

The effectiveness of POFA-GGBS systems is influenced by the choice of secondary binders. In combinations with OPC, POFA moderate's hydration kinetics while supporting strength development and chemical resistance [20, 24, 25]. PLC, with its reduced clinker content, benefits from POFA's filler effect and pozzolanic activity below a 10% replacement value , making it a viable alternative to traditional SCMs [26].

In contrast, NHL and CL present challenges due to their lower hydraulic activity and slower strength gain. However, POFA has potential to compensate for these limitations by supplementing pozzolanic reactions, improving early-age strength and expanding the structural viability of lime and aluminosilicate-based systems [27].

Experimental work shows that binary blending POFA with GGBS markedly improves the mechanical behaviour of AAMs in general, and geopolymers in particular. While AAMs encompass a broad class of binders produced by activating aluminosilicate precursors with alkaline solutions, geopolymers represent a specific subset characterised by a three-dimensional aluminosilicate network. Both systems demonstrated adequate compressive and tensile strengths, consistent workability, and a lowered CO_2e footprint [28-30].

The present study expands this evidence to examine POFA-GGBS mixtures incorporated into conventional calcium binders, Portland cements and limes, demonstrating how POFA-GGBS interacts with different calcium sources to influence strength development, setting and durability. Results support tailoring low-carbon, regionally adaptable concrete formulations by selecting appropriate cement or lime types and POFA-GGBS ratios to meet specific structural, environmental, and material availability constraints.

Despite increasing scholarly interest in SCMs, the academic representation of POFA within the context of Blast-Furnace cement remains markedly limited. A bibliometric analysis conducted across major databases yielded only 58 publications from a nested search of "Palm Oil Fuel Ash" within "Blast Furnace Cement", of which just 33 were suitable for scrutiny after accounting for duplicates, missing entries, and language barriers [31-63]. Of these, only three studies reported POFA chemical composition seven detailed its proportioning in concrete, and merely two explored its combination with GGBS, with none fulfilling all three criteria simultaneously [33,34,45,47,49,51,55]. The corpus comprised predominantly journal articles, including nine reviews, alongside a small number of theses, technical papers, and book chapters. Notably, 70% of the published works have emerged since 2020, indicating a recent surge in research activity. However, chemical composition data remain sparse and inconsistent, with only one paper providing original sample data.

Many scholars have examined the chemical composition of POFA, Table 1, understandably showing considerable variation, attributable to variations in pyro processing temperature, kiln retention times and precursor material combinations.

Table 1: Composition of POFA from Literature

References	SiO_2	CaO	Al_2O_3	Fe_2O_3	K_2O	MgO	Na_2O	SO_3	L.O.I
[24, 64]	43.60	8.40	11.40	4.70	3.50	4.80	0.39	2.80	18.00
[65]	63.60	7.60	1.60	1.40	6.90	3.90	0.10	0.20	9.60
[66]	53.82	4.24	5.66	4.54	4.47	3.19	0.10	2.25	10.49
[23]	61.85	5.09	5.65	5.45	5.09	2.79	0.10	0.28	9.88
[23]	67.09	5.58	6.12	5.92	5.45	3.06	0.11	0.32	2.20
[20,67]	58.30	6.72	6.69	9.77	8.40	3.69		0.96	7.34
[67]	59.60	8.06	7.05	8.77	7.64	3.09		0.57	14.85
[67]	52.50	11.30	8.83	5.73	10.20	3.55		0.82	6.72
[68]	51.18	6.93	4.61	3.42	5.52	4.02	0.06	0.36	21.60
[68]	65.01	8.19	5.72	4.41	6.48	4.58	0.07	0.33	2.53
[69]	59.17	5.80	3.73	6.33	8.25	4.87	0.18	0.72	16.10
[28, 29]	63.41	4.34	5.55	4.19	6.33	3.74	0.16	0.91	6.20
[70]	64.90	5.64	7.96	6.78	7.87	1.74		0.83	
[71]	53.50	8.30	1.90	1.10	6.50	4.10		2.70	20.90
[72]	62.50	19.00	4.50	3.12	2.00			0.53	
[73]	64.17	5.80	3.73	6.33	5.56	3.46		0.74	11.56
[74]	51.18	6.93	4.61	3.42	5.52	4.02	0.06	0.36	15.34
[74]	65.01	8.19	5.72	4.41	6.48	4.58	0.07	0.33	2.53
[75]	54.80	14.00	7.24	4.47		4.14		0.71	8.50
[76]	64.47	4.70	2.63	5.23	7.55	3.67	0.18	0.82	15.80

Across the literature, POFA exhibits considerable compositional variability, with silica content ranging from 43.6% to 67.1% by mass, a combined mean of lime, alumina, and silica at 72.3%, and loss on ignition (L.O.I) values spanning from 2.2% to 21.6%. These disparities are attributable to differences in pyro-processing conditions and precursor materials, emphasising the need for more rigorous and standardised investigations into POFA's role in blast furnace cement systems.

The high silica and alumina can react with calcium hydroxide during the hydration process of cement, pozzolanically, to form additional calcium silicate hydrate (C-S-H) gel. This can lead to an increase in the strength and durability of concrete.

The high L.O.I suggests high amounts of unburned carbon compounds in the ash likely caused by low temperature burning [74].

Hamada et al., performed a review of the current state of the use of POFA in concrete in 2018 and compared the chemical compositions of 44 samples from literature. Similarly, Amran et al., performed a critical review of POFA-based concrete and examined the composition of 27 POFA samples from literature [18, 76, 77]. Both these reviews agree with this study's literature review which updates prior research and contributes to extant knowledge regarding, the primary compound compositions and L.O.I range.

However, both the literature reviews and the literature examined in this study show limitations in compositional characterisation methodologies, suggesting that the current understanding of POFA is constrained by reliance on bulk oxide analyses, typically obtained through XRF or SEM-EDS, without complementary phase identification by XRD. As a result, the mineralogical assemblages, crystalline versus amorphous content, and the specific reactive phases within POFA remain poorly resolved. This gap restricts the ability to accurately predict pozzolanic reactivity, durability contributions, and long-term performance in blended binder systems, underscoring the need for integrated chemical and mineralogical characterisation in future investigations.

Recent reviews have extensively examined the incorporation of POFA as a SCM in both OPC and geopolymer concrete systems [18, 77-83]. These studies consistently highlight several beneficial effects associated with POFA utilisation, including enhanced material characteristics resulting from finer particle sizes, the development of a denser microstructure and notable improvements in compressive strength [18, 77, 79, 80, 82-84]. Additionally, POFA has been shown to delay hydration processes, improve resistance to sulphate attack, acid exposure, and carbonation, as well as reduce chloride ion penetration [78, 80, 83, 84]. From an environmental perspective, its use contributes to sustainable construction practices by valorising agro-waste materials [77, 81, 82, 84]. Despite these advantages, the literature presents some contradictory findings. For instance, POFA has been reported to both increase and decrease shrinkage , reduce and increase water absorption , and enhance or impair workability[18,78-80, 83]. These inconsistencies underscore the need for further systematic investigation to clarify the influence of POFA under varying mix designs and curing conditions.

Importantly, the pozzolanic activity of POFA is directly influenced by its particle fineness, amorphism, and content of both major and minor oxides, which can all be tuned through pre-treatment processes.

Experimental Preparation and Sample Production

The experimental programme encompassed the systematic preparation, production, curing, and evaluation of concrete specimens. During the preparation phase, chemical composition

and particle size distribution of the constituent materials were characterised [85]. Workability assessments were conducted during the production stage , while the cured composites were subsequently subjected to a series of mechanical and physical tests, including density measurements , flexural strength evaluation , and compressive strength testing using standard cube specimens [86-89].

The binder replacement was performed to replace equal parts GGBS and the secondary binder material. All mixes were produced to a 1:3 binder to aggregate mass ratio, whereby the aggregates were subdivided in to a 1:2 ratio of fine to coarse aggregate, giving the common concrete mix ratio of 1:1:2. The water to binder ratio (w/b) for all mixes was 0.4, resulting in variability in consistency and workability explored via slump testing.

All samples were subjected to the same initial conditions and demoulding process, upon which samples were separated with the majority submerged in water for testing at 7, 14, 28, and 91 days, with others left in ambient conditions in the laboratory for 28 and 91 days of curing to investigate the effects of carbonation on the concrete.

Material Characterisations

The NHL5 used, manufactured by Secil in Portugal, adhered to BS EN 459-1:2015 [90]. The GGBS adhered to BS EN 15167-1:2006 , manufactured in Scunthorpe UK by LKAB[91]. Both the NHL5 and the GGBS have been found to be representative of that found in literature [92]. The CEMI 52.5R and the CEMII/A-L 32.5R cements were produced by Cemex in Rugby UK to BS EN 197-1:2011 [93].

The materials used were subjected to chemical composition characterisation by way of X-ray fluorescence spectrometry (XRF) and X-ray diffraction (XRD), Table 2 and Table 3.

Table 2: Oxide Analysis of Constituent Minerals by X-ray Fluorescence Spectrometry (XRF)

	NHL5	GGBS	CL90	CEMI	CEMII	POFA
Amorphous oxide analysis (weight %)						
SiO_2	16.9	39.4	2.22	25.2	17.0	2.45
Al_2O_3	4.62	11.1	1.91	3.18	3.68	4.70
Fe_2O_3	2.92	0.31	<0.1	0.32	3.45	0.39
CaO	71	44.7	93.6	67.1	70.4	1.44
MgO	1.38	1.46	0.97	1.33	1.19	1.18
K_2O	0.83	0.43	0.27	0.30	0.66	47.2
Na_2O	0.18	0.11	0.25	<0.1	<0.1	<0.1
SO_3	1.35	1.49	0.11	1.57	2.61	18.7
P_2O_5	<0.1	<0.1	<0.1	0.11	<0.1	<0.1
Cl	<0.1	<0.1	<0.1	0.23	0.19	23.3
L.O.I	18.8	0.2	25.5	5.26	8.79	23.3

N.B. L.O.I. performed at 975°C

Table 3: Crystalline Mineral Phases by X-ray Diffraction (XRD)

	NHL5	GGBS	CL90	CEMI	CEMII	POFA
Crystalline compound analysis (weight %)						
Calcium Carbonate ($CaCO_3$)	38.7	100	4.5		19.7	
Calcium Hydroxide ($Ca(OH)_2$)	28.7		95.5			
Calcium Silicate (Ca_2SiO_4)	28.4			15.0	2.5	
Silicon Oxide (SiO_2)	4.1					
Tricalcium silicate (Ca_3SiO_5+$Ca_3(SiO_4)O$)				68.0	40.7	
Tricalcium aluminate ($Ca_3Al_2O_6$)				13.3	25.4	
Brownmillerite ($Ca_4Al_2Fe_2$+$3O_{10}$)				1.8	4.5	
Gypsum ($CaSO_4 \cdot 2H_2O$)				1.1	1.1	
Anhydrite ($CaSO_4$)				0.8	6.1	
Ammonium Potassium Sulphate						
$((NH_4)_{0.104}K_{1.896})(SO_4)$						37.3
Potassium Chloride (KCl)						62.7

N.B. GGBS sample mostly amorphous

The POFA material studied is distinct from that found in literature, with all but lime, alumina, and sodium hydroxide being outside of two standard deviations of that for the elemental analysis from literature.

Most notably, four issues arise: firstly, the combination of the primary oxides for pozzolanic reactivity and contribution being lime, alumina and silica total 8.64% mass, too low to be considered a pozzolan; secondly, the L.O.I is extremely high at 89.2% suggesting considerable combustible material is present, such as undesirable organics; thirdly, the potassium oxide content, although typically high in POFA, is near five times that found in literature at 47.2%; and finally, the sulphur trioxide content is extremely high at 18.7%.

When evaluating the crystalline phases by way of XRD, Table 3, two compounds are evident being ammonium potassium sulphate and potassium chloride which corroborate the high L.O.I, SO_3 and K_2O as these salts are volatile and hygroscopic. Together, these aspects suggest very low pozzolanic potential, due to contamination or dilution by other phases and processing.

Particle size distributions were taken of the component materials for comparison, Figure 1, showing that the cements, limes and PCRs fell into the particle sizes typical of fines and fillers. However, notably some of the POFA contributed to the particle size range of the fine aggregate.

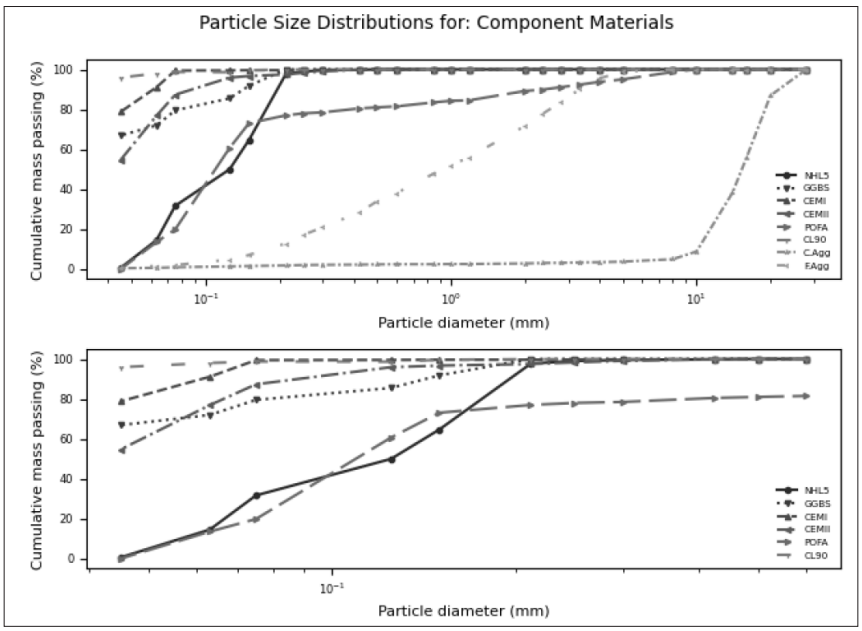

Figure 1: Particle Size Distributions of Component Materials

Two distinct particle types where visible during sieving of the POFA, grey/white fine particulate matter and black short strands, Figure 2. The black strands were most evident between 600 -150µm and not present on the 125µm sieve or below. This coincides with the point of gradient change noticeable in the PSD for POFA where a distinct split can be made between 27% of the material being well graded over 150µm to 8mm and the remaining 73% of the material being in the narrow range of 45-150µm, following a similar distribution to that of NHL5 from 150µm down. The particle sizes of the cements, GGBS and hydrated lime were all significantly smaller, with CL90 the finest material.

Figure 2: Sieves Containing Two Distinct Particle Types

The aggregates used in this study were identical across the testing groups with the aggregate to binder ratios being maintained throughout. Both the fine and coarse aggregates have been characterised in a previous study both adhering to BS 12620:2013 being identified as GF85f3 and Gc85/15f1, respectively [92,94].

Sample Production

Two high volume GGBS proportions of 90/10 and 80/20 were compared for four distinct secondary binders including two types of limes and two common cements. Further, for those combined at GGBS being 80% of the total binder mass, were replaced in equal parts by POFA at 1% increments up to 6% binder mass replacement. These were also compared to controls of 100% CEMI and 100% CEMII binders and both with 3% mass replacement with POFA, resulting in the binder combinations outlined in Table 4, with all mixes being of a 1:1:2 aggregate ratio at 0.4w/b.

Table 4: Binder Combinations

Mix ID	Binder Mass (%)						Slump (mm)	Slump Class
	GGBS	POFA	CEMI	CEMII	NHL5	CL90		
CEMI	0.0	0.0	100.0	0.0	0.0	0.0	35	S1/S2
CEMI PA3	0.0	3.0	100.0	0.0	0.0	0.0	100	S2/S3
CEMI GGBS 10/90	90.0	0.0	10.0	0.0	0.0	0.0	35	S1/S2
CEMI GGBS 20/80	80.0	0.0	20.0	0.0	0.0	0.0	30	S1
CEMI GGBS 20/80 PA1	79.5	1.0	19.5	0.0	0.0	0.0	20	S1
CEMI GGBS 20/80 PA2	79.0	2.0	19.0	0.0	0.0	0.0	50	S1/S2
CEMI GGBS 20/80 PA3	78.5	3.0	18.5	0.0	0.0	0.0	75	S2
CEMI GGBS 20/80 PA4	78.0	4.0	18.0	0.0	0.0	0.0	80	S2
CEMI GGBS 20/80 PA5	77.5	5.0	17.5	0.0	0.0	0.0	50	S1/S2
CEMI GGBS 20/80 PA6	77.5	5.0	17.5	0.0	0.0	0.0	50	S1/S2
CEMII	0.0	0.0	0.0	100.0	0.0	0.0	100	S2/S3
CEMII PA3	0.0	3.0	0.0	100.0	0.0	0.0	90	S2/S3
CEMII GGBS 10/90	90.0	0.0	0.0	10.0	0.0	0.0	80	S2
CEMII GGBS 20/80	80.0	0.0	0.0	20.0	0.0	0.0	70	S2
CEMII GGBS 20/80 PA1	79.5	1.0	0.0	19.5	0.0	0.0	50	S1/S2
CEMII GGBS 20/80 PA2	79.0	2.0	0.0	19.0	0.0	0.0	90	S2/S3
CEMII GGBS 20/80 PA3	78.5	3.0	0.0	18.5	0.0	0.0	60	S2
CEMII GGBS 20/80 PA4	78.0	4.0	0.0	18.0	0.0	0.0	50	S1/S2
CEMII GGBS 20/80 PA5	77.5	5.0	0.0	17.5	0.0	0.0	60	S2
CEMII GGBS 20/80 PA6	77.0	6.0	0.0	17.0	0.0	0.0	50	S1/S2
NHL GGBS 10/90	90.0	0.0	0.0	0.0	10.0	0.0	30	S1
NHL GGBS 20/80	80.0	0.0	0.0	0.0	20.0	0.0	10	S1
NHL GGBS PA1	79.5	1.0	0.0	0.0	19.5	0.0	40	S1/S2
NHL GGBS PA2	79.0	2.0	0.0	0.0	19.0	0.0	50	S1/S2
NHL GGBS PA3	78.5	3.0	0.0	0.0	18.5	0.0	40	S1/S2
NHL GGBS PA4	78.0	4.0	0.0	0.0	18.0	0.0	35	S1/S2
NHL GGBS PA5	77.5	5.0	0.0	0.0	17.5	0.0	45	S1/S2
NHL GGBS PA6	77.0	6.0	0.0	0.0	17.0	0.0	40	S1/S2
CL90 GGBS 10/90	90.0	0.0	0.0	0.0	0.0	10.0	30	S1
CL90 GGBS 20/80	80.0	0.0	0.0	0.0	0.0	20.0	20	S1
CL90 GGBS PA1	79.5	1.0	0.0	0.0	0.0	19.5	10	S1
CL90 GGBS PA2	79.0	2.0	0.0	0.0	0.0	19.0	10	S1
CL90 GGBS PA3	78.5	3.0	0.0	0.0	0.0	18.5	20	S1
CL90 GGBS PA4	78.0	4.0	0.0	0.0	0.0	18.0	20	S1
CL90 GGBS PA5	77.5	5.0	0.0	0.0	0.0	17.5	20	S1
CL90 GGBS PA6	77.0	6.0	0.0	0.0	0.0	17.0	30	S1

Concrete mixes corresponding to the 36 combinations were produced to form 100mm cube samples and 100x100x150 prisms for compressive and flexural testing, respectively. Around 600 samples were produced over four production sessions. Once the initial

set was completed the samples were demoulded and placed into two curing conditions.

Curing Regimes

To investigate the effects of curing conditions on compressive strength, all specimens underwent a standardised initial curing regime for three days prior to demoulding. Following demoulding, a portion of the samples was immersed in water maintained at 16 ± 3 °C, while the remaining samples were subjected to air curing under controlled laboratory conditions (20 ± 5 °C, 50 ± 10% relative humidity) for the subsequent intervals of 7, 14, 28, and 91.

Results and Discussion

The experimental programme yielded significant insights into the mechanical behaviour of concrete incorporating POFA and high-volume GGBS binders. By systematically varying POFA content and evaluating four secondary cementitious materials under controlled curing regimes, the study elucidates the influence of binder composition and curing environment on the development of compressive and flexural strength across multiple curing ages.

Chemistry Comparison

The chemical composition of the POFA examined in this study differs substantially from values reported in the literature, Table 1. Published data typically describe POFA as a silica-rich material, with SiO_2 contents of approximately 43-67 mass %, moderate CaO (4-19 mass %), and relatively low alkali and sulphate contents. In contrast, XRF analysis of the present sample, Table 2, revealed exceptionally low SiO_2 (2.45 mass %) and CaO (1.44 mass %), coupled with extremely high K_2O (47.2 mass %) and SO_3 (18.7 mass %). The L.O.I was also unusually high at 89.2 mass %, far exceeding the 2-22 mass % range typically reported, indicating a substantial proportion of volatile matter.

XRD analysis, Table 3, confirmed that the crystalline phases are dominated by potassium chloride (62.7 mass %) and ammonium potassium sulphate (37.3 mass %), with no detectable crystalline silica or calcium silicate phases. This mineralogical profile contrasts sharply with conventional POFA, which often contains quartz, cristobalite, or amorphous silica phases that contribute to pozzolanic reactivity. The high soluble salt content explains the elevated K_2O and SO_3 values and is likely to influence performance in cementitious systems, potentially increasing the risk of efflorescence, altering setting behaviour, and limiting long-term strength development.

These pronounced compositional and mineralogical differences suggest that the POFA investigated here is unlikely to exhibit the pozzolanic performance typically associated with this material in the literature. Pre-treatment methods such as washing or controlled calcination may be required to remove soluble salts, reduce L.O.I, and concentrate reactive silica before its effective use as an SCM.

The divergence from silica-rich POFA compositions reported previously is likely attributable to a combination of factors:

- contamination from fertiliser residues or soil adhering to palm fruit bunches prior to combustion, consistent with the exceptionally high K_2O and SO_3 contents and the dominance of potassium chloride and ammonium potassium sulphate phases;
- incomplete combustion or low-temperature burning, as indicated by the very high L.O.I, which would preserve volatile salts and unburnt organic matter while limiting the formation of reactive amorphous silica;
- inherently low silica content in the feedstock or dilution by non-ash material during collection, explaining the absence of crystalline silica phases in the XRD profile; and
- post-combustion handling and storage effects, particularly exposure to moisture or mixing with boiler deposits, which could further concentrate soluble salts and reduce the relative proportion of reactive oxides.

Collectively, these factors indicate that the POFA in this study is chemically and mineralogically distinct from conventional POFA, and its direct incorporation into cementitious systems is unlikely to replicate the performance reported in previous research without prior processing to remove soluble salts and enhance reactive silica content.

The presence of ammonium potassium sulphate as a soluble salt constituent of the POFA used in this study has significant practical and durability implications for concrete production and performance. Soluble sulphate increases the effective sulphate availability in fresh paste and can promote ettringite formation in the presence of reactive aluminates and sufficient moisture, with potential consequences for early-age expansion, setting behaviour and delayed ettringite formation (DEF) [95, 96]. Conversely, modest additional sulphate may mitigate rapid set by complexing with aluminates dependent on speciation, so the net effect is dependent on both concentration and overall system chemistry [97,98].

The ammonium fraction is highly mobile and prone to leaching [99]. Leachable ammonium and potassium ions elevate pore solution ionic strength and may trigger admixture-sensitive reactions, most notably those associated with OH- availability [100]. Potassium ions contribute to the alkali inventory of the binder system, increasing the alkali loading relevant to alkali-silica reaction (ASR) risk; increments in soluble potassium ions (K^+) can be significant in low-alkali binders or when reactive aggregates are present [101]. High concentrations of soluble salts can also increase water demand and alter the performance of admixtures through competitive adsorption or ionic strength effects , thereby affecting fresh rheology and admixture dosing requirements [102].

Elevated potassium chloride (KCl) content in the POFA further compounds these concerns. Soluble KCl increases the readily available alkali and chloride inventories in the pore solution, thereby elevating the risk of ASR in the presence of reactive aggregates and promoting reinforcement corrosion in chloride-sensitive environments [103].

Although no universal critical chloride threshold (CCT) has been established for the de-passivation of the steel reinforcement's protective film as it is dependent on both: cement chemistry, including pore solution alkalinity, pore size and moisture content and the steel, including grade and surface profile/condition [104]. Commonly it is reported at 0.2-1 binder wt% or at a 0.6 ratio of chloride to hydroxyl ion activity [104, 106], with the current limits are set at 0.1-1 binder wt % in BS8500-1, specifically 0.4% binder wt% for general reinforced concrete in XS or XD exposure classes [105-107].

However, the combined influence of coexisting alkali sulphate salts and chlorine exposure remains insufficiently understood and represents a pertinent research gap [108, 109]. Both effects are concentration-dependent and particularly critical in low-alkali binder systems or where cover and exposure conditions demand

strict chloride limits [109]. Soluble chlorides can also influence early hydration and setting behaviour via ionic strength effects and reduce the efficiency of polycarboxylate superplasticisers through competitive adsorption or electrolyte screening, with associated impacts on workability and admixture dosing [102,110]. High soluble K^+ and Cl^- contents may also promote leaching and efflorescence , compromise or benefit freeze-thaw resistance, if not explicitly accounted for, by altering pore solution chemistry and confound durability assessments [109,111,112].

To manage these risks, POFA batches containing appreciable KCl should be analysed for water-soluble chloride and alkali content, and appropriate mitigation measures implemented. These may include limiting POFA replacement levels, blending with low-alkali or chloride-binding SCMs, applying corrosion inhibitors or sacrificial anodes, and/or pre-treating the POFA (e.g., washing or thermal treatment) to remove soluble salts.

PSD Analysis of the POFA Sample Revealed two Distinct Morphologies:

- A light grey, fine powder fraction, and
- Fine, fibrous or strand-like particles. The light grey powder is likely composed of the finer mineral ash fraction, potentially containing residual amorphous or crystalline phases, whereas the fibrous strands may represent incompletely combusted organic matter or elongated salt crystallites formed during cooling.

This bimodal morphology is consistent with the high L.O.I of 89.2 mass % and the dominance of soluble salts identified by XRD. The fibrous fraction may contribute disproportionately to the L.O.I through its organic content or volatile salt phases, while the powder fraction is more likely to contain the limited mineral oxide phases present. The coexistence of these two particle types suggests incomplete combustion and heterogeneous feedstock processing, which could result in variable reactivity, water demand, and workability in cementitious systems.

From a practical standpoint, the fibrous strands may act as inert inclusions, reducing packing density and potentially increasing porosity, while the fine powder fraction could influence early hydration kinetics through its high soluble salt content. Pre-treatment steps such as sieving, milling, or washing could be employed to remove or reduce the fibrous fraction, thereby improving the uniformity and performance predictability of the POFA when used as a SCM.

The chemical and mineralogical characteristics of the POFA, marked by exceptionally high K_2O (47.2 mass %), dominant crystalline phases of KCl (62.7 mass %) and (NH4)KSO4 (37.3 mass %), and very low CaO (1.44 mass %) and SiO_2 (2.45 mass %), are consistent with a volatile-enriched fine fraction analogous to cement kiln bypass dust, but originating from palm oil biomass combustion. In cement manufacture, bypass dust is removed from the kiln gas stream to prevent the recirculation of volatile salts similarly, in biomass systems, fine particulate capture (e.g., via cyclones, bag filters, or electrostatic precipitators) can yield a salt-rich dust stream distinct from the bulk bottom ash, alongside having considerable variability in composition due to: biomass feedstock; pyrolysis temperature; pre- and post-processing, such as washing [113,114]. The composition of the present sample suggests it represents such a fraction, enriched in highly soluble alkali chlorides and sulphates through volatilisation-condensation processes during combustion and subsequent gas cooling.

This volatile-rich nature explains its divergence from the silica-rich POFA commonly reported in the literature and indicates that, in its untreated state, it would behave primarily as a high-alkali, high-chloride admixture rather than as a reactive pozzolan. Its direct incorporation into cementitious systems would therefore carry significant risks for durability, setting behaviour, and admixture compatibility, unless pre-treated to remove soluble salts and concentrate reactive silica. This classification also helps explain the divergence between the mechanical and durability performance observed in this study and that reported for conventional, silica-rich POFA, as the potash-like composition of the present material, dominated by soluble potassium and chloride salts, means it functions primarily as a chemical admixture rather than as a pozzolanic ash.

Furthermore, the volatile-rich, salt-dominated chemistry of the POFA is congruent with the early and abundant formation of mixed chloro-sulphate AFm phases, particularly Kuzel's salt, in blended cement-GGBS systems, driven by the simultaneous high availability of Cl^- and SO_4^{2-} in the presence of reactive aluminates and carbonates.

Kuzel's Salt (Ca4Al2(SO4)1/2Cl(OH)12·5H2O) is part of the layered double hydroxide (LDH) family with positively charged main layers [Ca2Al(OH)6]+ and negatively charged interlayers $[Cl0.5\cdot(SO_4)_{0.25}\cdot 2.5H_2O]-$, with Independent chloride and sulphate anions in separate crystallographic sites [115].

In blended binders containing PLCs and/or NHLs, the additional $CaCO_3$ introduced into the system increases carbonate availability in the pore solution, favouring the formation of mono- and hemicarbonate AFm phases. In chloride-rich environments, reactive aluminates from clinker and SCMs such as GGBS can instead promote the precipitation of Friedel's salt, with Kuzel's salt forming transiently where sulphate is also present. The stability of these chloride-bearing AFm phases is governed by the competitive incorporation of CO_3^{2-}, Cl^-, and SO_4^{2-} into the AFm interlayers, with high carbonate activity potentially displacing chloride and reducing long-term chloride binding capacity. This dynamic equilibrium between carboaluminate, chloroaluminate, and chloro-sulphoaluminate phases has important implications for chloride ingress resistance, as shifts in pore solution chemistry over time can alter both the quantity and stability of bound chlorides.

The simultaneous high availability of Cl^- and SO_4^{2-} from KCl and $(NH_4)KSO_4$, in combination with reactive aluminates from clinker and GGBS, creates conditions that favour the early formation and stability of Kuzel's salt during hydration [115]. Elevated K^+ concentrations may enhance GGBS activation even more so than Na^+ however, pre-saturation of AFm phases with chloride reduces their capacity to bind additional chlorides, increasing the risk of reinforcement corrosion [116,117]. The low CaO content of the POFA means that $Ca(OH)_2$ generation is dependent on other binder components, while the high alkalinity of the pore solution will influence AFm solubility, ion-exchange processes, and long-term phase assemblage stability [117].

Resulting in a dichotomy whereby POFA can be both beneficial to concrete performance and detrimental to any underlying reinforcement.

Anecdotal Evidence

During the initial curing period, concrete specimens incorporating high POFA contents (>4 mass %) exhibited the formation of fine, white, strand-like efflorescence on the top surface, accompanied

by visible rusting and patina of the cast-iron moulds, Figure 3.

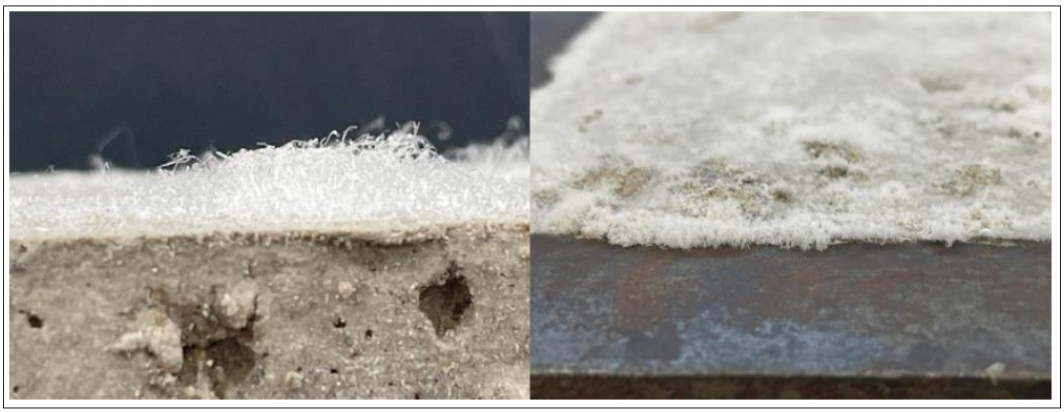

Figure 3: High POFA Content Efflorescence and Rusting

These phenomena provide direct, macroscopic evidence of the substantial soluble salt load introduced by the POFA. The migration of chloride- and sulphate-rich pore solution to the surface is consistent with the volatile-rich, salt-dominated composition identified by XRF/XRD, and with the classification of this material as a bypass/flue-dust-type fraction or potash fertiliser contaminant from biomass combustion. The corrosion of the moulds further indicates that aggressive ionic species, particularly chlorides, were present in sufficient concentration to de-passivate iron surfaces even under early-age curing conditions.

This behaviour aligns with the predicted hydration chemistry: the simultaneous high availability of Cl^- and SO_4^{2-} from KCl and $(NH_4)KSO_4$, in the presence of reactive aluminates from clinker and GGBS, would favour the rapid formation of mixed chloro-sulphate AFm phases, notably Kuzel's salt. However, the likelihood of migration to the surface for efflorescence is questionable.

Likely other efflorescent compounds including calcium carbonate ($CaCO_3$), calcium sulphate ($CaSO_4$), potassium carbonate (K_2CO_3), potassium sulphate (K_2SO_4), sodium sulphate (Na_2SO_4), calcium chloride ($CaCl_2$), KCl, are responsible.

The two phenomena of efflorescence and rust are clearly related, but the active mechanisms may involve different compounds. With calcium and potassium carbonates associated with efflorescence and their chlorides most associated with steel depassivation.

Ultimately efflorescence is an indicator of permeability and moisture conveyance. Capillary transport during early hydration can carry unbound salts to the surface, where they crystallise as efflorescence, while maintaining high chloride activity in the pore solution in contact with the moulds or potential reinforcing steel. Targeted characterisation of the effloresced material, via XRD, SEM-EDS, or ion chromatography, could confirm the unlikely presence of Kuzel's salt or other related AFm phases, providing a direct link between the material's unusual chemistry, its bypass/flue-dust-like origin, and its observed influence on early-age durability indicators.

These early-age signs of salt migration and corrosion underscore a critical durability concern: the rapid movement and crystallisation of chloride- and sulphate-rich salts both confirm the bypass/flue-dust-like chemistry of the POFA and foreshadow heightened long-term risks of reinforcement corrosion, surface scaling, and persistent efflorescence if used without pre-treatment to remove soluble salts. At the same time, they provide essential context for interpreting the subsequent results on workability, compressive and flexural strength, and the effects of different curing regimes, where the same volatile-rich, high-alkali, high-chloride chemistry is expected to exert a decisive influence on both fresh and hardened performance.

Workability

The workability testing followed BS EN 12350-2 , resulting in all mixtures being characterised between slump class 1 and 3, Table 4 [86]. The relationship of POFA inclusion differed for each highvolume GGBS systems, with three of the four showing a moderate increase in workability, and one, CEMII, showing a reduction in workability with increasing POFA, Figure 4.

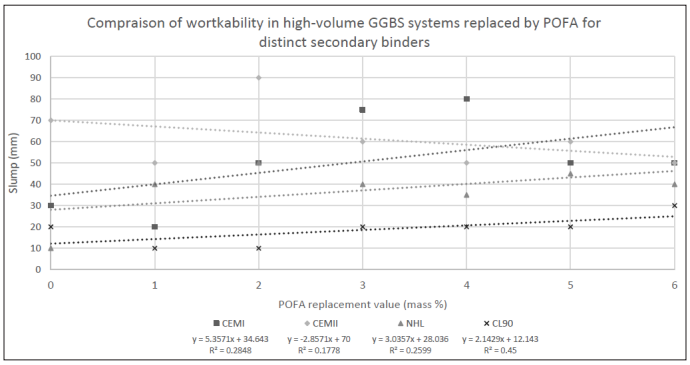

Figure 4: Workability Comparison of High-Volume GGBS Systems with POFA Inclusion

The slump data show clear grouping by binder type and by POFA inclusion. CEM I and CEM II systems without POFA generally occupy higher slump classes (S2-S3 or upper S1), whereas binary blends with high GGBS content, NHL and CL90 systems give markedly lower slumps (predominantly S1). Adding POFA produces both increases and decreases in slump depending on the host binder and GGBS proportion, indicating that POFA's effect on fresh rheology is contingent on the base cement chemistry and blend ratio.

Plain CEM I show low to moderate workability (35 mm, S1/S2). CEM II displays substantially higher slump (100 mm, S2/S3), indicating that the PLC or filler content in CEM II improves initial flow relative to pure CEM I.

For CEM I, the POFA at 3% replacement increases slump from 35 to 100 mm, Table 4, moving the mix from S1/S2 into S2/S3. For CEM II, POFA 3% replacement produces a small reduction from 100 to 90 mm but remains in S2/S3. These outcomes show that POFA can act as a lubricating microfiller in some cement matrices but that its effect is modulated by the existing chemistry of the binder.

Binary CEM I/GGBS mixes without POFA have low slumps (30-35 mm), reflecting the low water to binder ratio. Introducing POFA to CEM I/GGBS produces variable responses: some POFA levels further reduce slump (e.g., POFA 1% reducing 30 → 20 mm), others increase it markedly (POFA 3% 30 → 75mm). The same pattern appears for CEM II/GGBS where baseline slumps are higher (70-80 mm) and some POFA additions, POFA 2% increase slump to 90 mm, further improve flow while others reduce it. This variability implies that POFA particle characteristics (fineness, shape, absorption) and dosage interact with GGBS to alter packing and free-water availability.

NHL5/GGBS and CL90/GGBS systems yield the lowest slumps overall, concentrated in S1 (10-50 mm range). POFA additions in these systems produce minor, mostly downward or neutral shifts in slump. The low slumps reflect the lower intrinsic water demand tolerance and different chemistry of hydraulic lime (NHL5) and air lime (CL90) binders, where POFA's filler/absorption effects are insufficient to raise flow and may instead increase water demand. POFA can improve packing and reduce interparticle friction if its particles are fine and well-graded relative to the binder constituents, yielding higher slump. Conversely, coarse or porous POFA will increase water demand and reduce slump. The divergent responses across binders indicate that POFA's particle size distribution and porosity interact with the existing fines (GGBS, PLC, lime) to determine net packing efficiency.

The POFA utilised in this study, characterised by its coarse and broadly distributed particle size Figure 1, was anticipated to reduce workability across all binder systems. Contrary to this expectation, the experimental results, Figure 4, revealed an increase in workability, suggesting that the unique chemical composition of the POFA, particularly its elevated chloride and sulphate content, may play a significant role in modifying slump behaviour. These findings prompt further investigation into the mechanisms by which such mineral admixtures influence fresh-state properties.

Unlike well-graded fine fillers that improve particle packing and reduce interparticle friction, coarse, heterogeneous POFA particles neither efficiently fill interstitial voids nor contribute to a continuous lubricating film; instead, they increase the apparent paste requirement to wet particle surfaces, disrupt packing homogeneity and elevate water demand. However, these effects should be reduced in high-GGBS, NHL and low-clinker (CL90) blends, where the intrinsic high specific surface area and water affinity of the constituent powders already limit free water availability, such that replacement with coarse POFA improves slump but increases rheological variability.

Instances where POFA produced modest improvements in slump are attributable to specific combinations of binder chemistry and POFA fractionation in which the POFA provided a small proportion of suitably fine or rounded particles that enhanced slip between fines, Figure 2, and replaces finer materials that have potentially higher specific surface area.

Therefore, in general the non-uniform, coarse POFA PSD is expected to destabilise fresh concrete flow unless mitigated by particle-size refinement (milling or sieving), supplementation with fillers, or targeted adjustment of superplasticiser dosing to restore packing and preserve desired w/b ratios. Practical implications for mix design arising from these findings are threefold.

- First, the effect of POFA on fresh rheology is binder-dependent and cannot be generalised; therefore, POFA dosage should be calibrated for each specific binder/GGBS combination rather than assumed transferable across systems.
- Second, in inherently low-workability matrices such as NHL5/GGBS and CL90/GGBS, POFA is unlikely to provide meaningful improvements in flow, so designers should plan for supplementary measures to achieve target workability.
- Third, where POFA has been observed to enhance, there is potential to reduce superplasticiser demand or lower water content, offering material-efficiency and sustainability benefits provided that any reduction in admixture or w/b ratio is validated against mechanical and durability requirements.

Compressive Strengths

Primary OPC and PLC Systems with POFA Addition

All mixes exhibited progressive increases in compressive strength from 7 to 91 days, with the greatest rate of gain occurring between 7 and 28 days and a reduced rate thereafter.

CEMI mixes consistently achieved higher strengths at all ages than CEMII mixes, and the substitution of 3% POFA produced a modest early-age strength reduction in both cement types followed by partial recovery by 91 days, consistent with a delayed pozzolanic contribution.

The incorporation of 3% POFA results in adjusted 28-day compressive strengths for OPC and PLC concretes, Figure 5, with values of 10.4 and 9.2 MPa lower than their respective controls. The relative impact is proportionally greater for PLC (24%) compared to OPC (18%).

The CEMII, 3% POFA mixture showed the lowest absolute strengths and the slowest strength development, indicating a compounded dilution effect of limestone and POFA that limits early hydration and retards early strength gain. These trends suggest that the positive influence of POFA manifests primarily at later ages through secondary pozzolanic reactions that densify the matrix, while early-age performance remains governed by available clinker content.

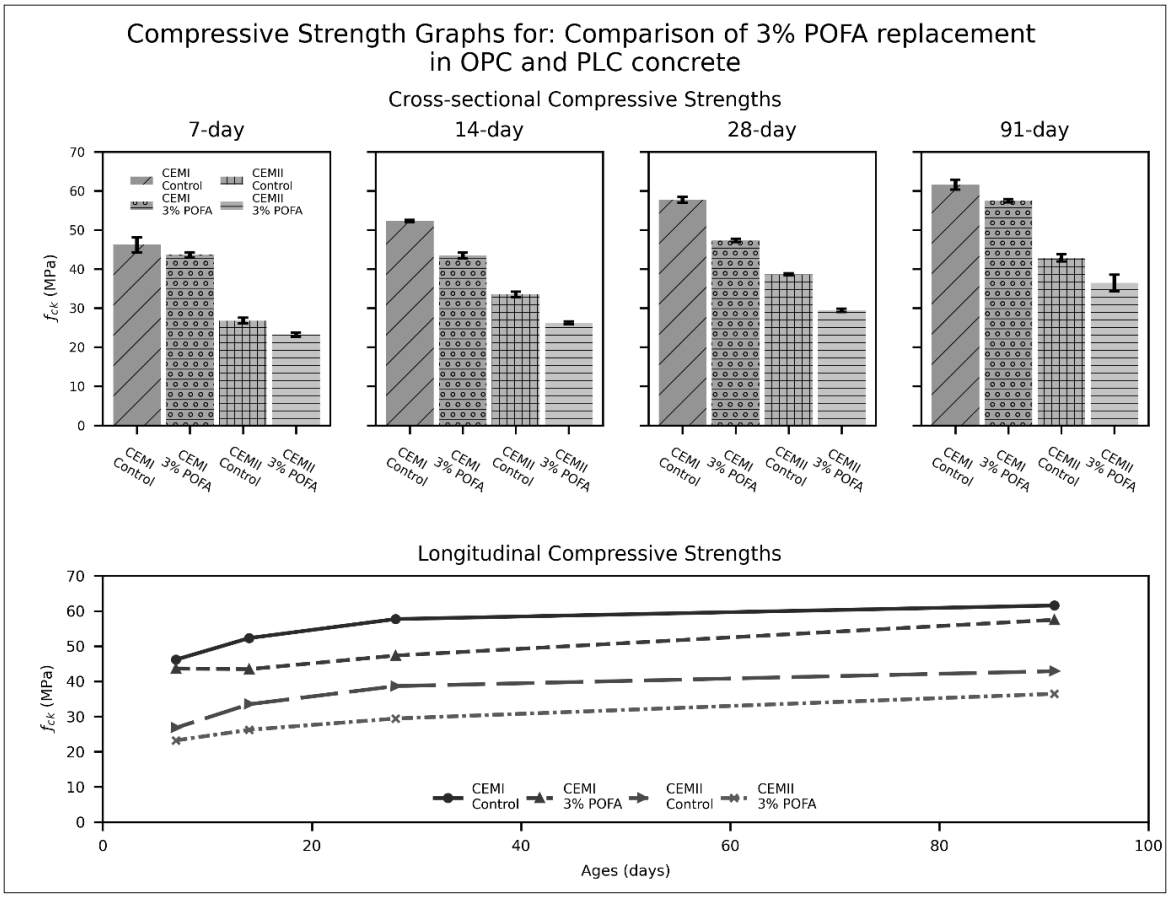

Figure 5: Comparison of Compressive Strength of 3% POFA Binder Replacement in OPC and PLC Concrete

The inclusion of 3% POFA in OPC and PLC concrete leads to reduced early-age compressive strength, as expected for a pozzolanic SCM with latent reactivity. The reduction is mild at such low dosage but remains consistently measurable.

Despite conventional expectations, the unique chemistry of the POFA used in this study challenges the typical explanation for late-age strength recovery.

Traditionally, such recovery is attributed to the gradual pozzolanic activity of POFA, wherein its amorphous silica reacts with available $Ca(OH)_2$ in the presence of sustained moisture. However, the presence of potassium chloride and potassium ammonium sulphate in this POFA sample introduces alternative mechanisms that may better explain the observed behaviour.

These soluble salts can enhance ionic strength in the pore solution, promoting particle dispersion and improving initial workability, contrary to expectations based on particle size alone. Additionally, chloride ions may accelerate early hydration reactions, while ammonium ions could influence pore structure and moisture retention. Sulphate contributions may further stimulate ettringite formation, affecting both early and long-term strength development. In practice, OPC-POFA blends often approach control strength values by 91 days, while PLC-POFA systems exhibit less complete recovery, though they remain structurally viable under optimal curing conditions.

The principal mechanisms influencing long-term strength development include:
- initial dilution of reactive clinker phases;
- delayed formation of secondary C-S-H through pozzolanic reaction;
- reduced portlandite availability in blended systems; and
- the interplay of pore structure, moisture retention, and curing regime, now further complicated by the ionic effects of the POFA's unique composition.

Binary GGBS-Dominant Systems

All binary GGBS systems demonstrated monotonic increases in compressive strength with curing age, with the most pronounced gains observed between 7 and 28 days, followed by a reduced rate of increase from 28 to 91 days.

Mixtures containing higher cement proportions, specifically CEM I/GGBS 20/80 and CEM II/GGBS 20/80, consistently achieved superior early and intermediate-age strengths compared to higherGGBS blends of 10/90.

NHL/GGBS systems exhibited slower early-age strength development but showed appreciable gains at later ages, indicating a delayed hydraulic contribution.

High-volume GGBS mixtures displayed heightened sensitivity to further OPC and PLC substitution beyond 80%, as evidenced by reductions in 28-day compressive strength of 9.8 MPa and 11.7 MPa, respectively, Figure 6.

A similar trend was observed for NHL5-based systems, which experienced a 24.7% reduction in 28day strength. In contrast, hydrated lime (CL90) blends showed a modest increase of 1.46 MPa in 28day strength when GGBS content was increased from 80% to 90%, corresponding to an 8.2% improvement.

Differences between CEM I- and CEM II- GGBS systems were relatively minor, attributable to variations in clinker content and limestone dilution that affect early hydration kinetics. Notably, CL90GGBS combinations were the only system to exhibit improved compressive strength with reduced secondary binder content, suggesting that further replacement of GGBS by CL90 beyond 10% is detrimental to mechanical performance.

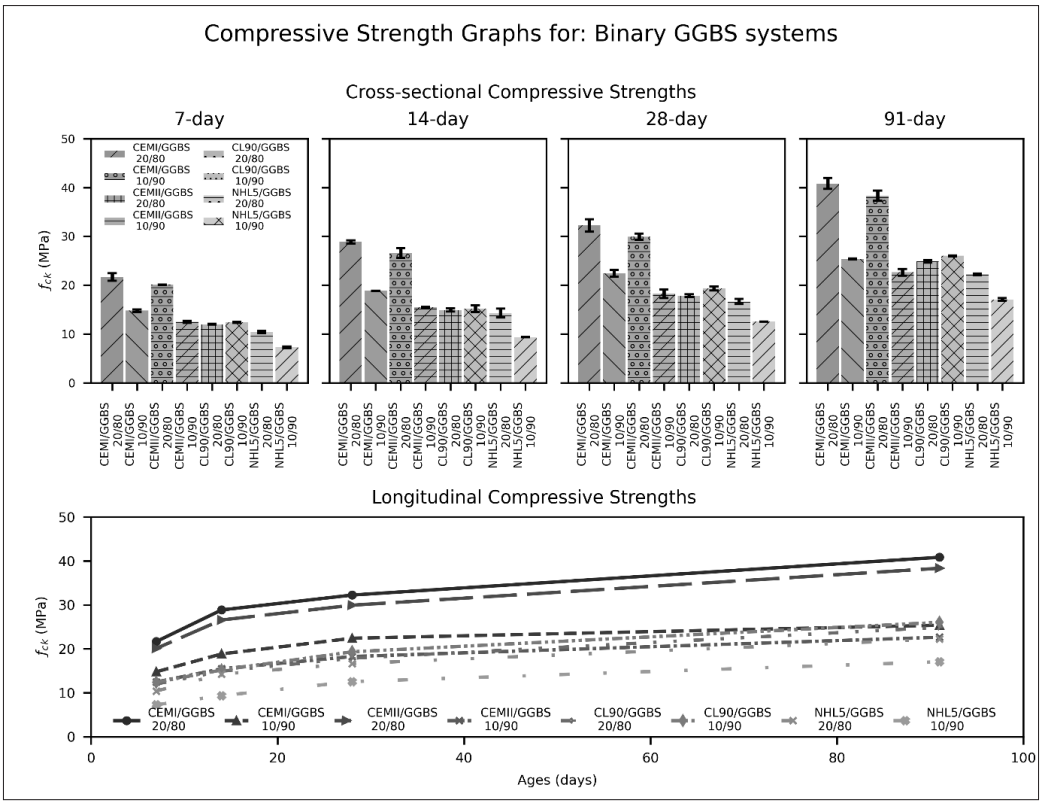

Figure 6: Compressive Strength of High Volume GGBS Cementitious Systems

The compressive strength development in binary GGBS systems is defined by a balance between reduced initial hydration kinetics and profound late-age strength and durability gains. While cement systems such as CEM I/GGBS and CEM II/GGBS maintain high performance up to ~60% [6], ~40% , GGBS replacement respectively, further increases result in accelerated 28-day strength decline, only partially offset by late-age recovery [118].

NHL/GGBS based systems increase performance up to ~60-70% proportions of GGBS decreasing thereafter, with high GGBS contents (>80%) crossing a threshold beyond which strength rapidly diminishes and a 24.7% reduction in characteristic 28-day compressive strength (fck) signalling suboptimal combination [92].

In agreement with literature, considerable, utilisable compressive strength is achievable with binary CL90/GGBS binder systems in concrete [10]. Conversely to the other systems studied, in CL90/GGBS systems reducing the CL90 fraction below 20% improves early strength, suggesting an optimum activator-to-slag ratio exists for maximising C-S-H formation and matrix densification at a high proportion of GGBS.

The unique hydration behaviours, microstructural outcomes, and temporal strength progression of these binary systems reinforce the necessity of application-specific mix design, emphasising adequate curing, careful optimisation of secondary binder ratios, and a nuanced understanding of long-term performance as codified in the revised concrete standard [107]. However, this standard still leaves room for improvement, with many complex novel combinations absent, including those that incorporate POFA.

High-Volume GGBS Binary Systems with POFA Replacement

Ordinary Portland Cement and Ground Granulated Blast Furnace Slag

Contrary to the primary OPC system, within the CEMI/GGBS system the addition of POFA can be seen to have a positive influence on the compressive strength development at all replacement values at an early age under water curing up to 91 days, where at 1-4% replacement gains can be seen at all ages, reducing at 5% and 6% replacement samples near equal to that of the control by 91-days of curing, Figure 7.

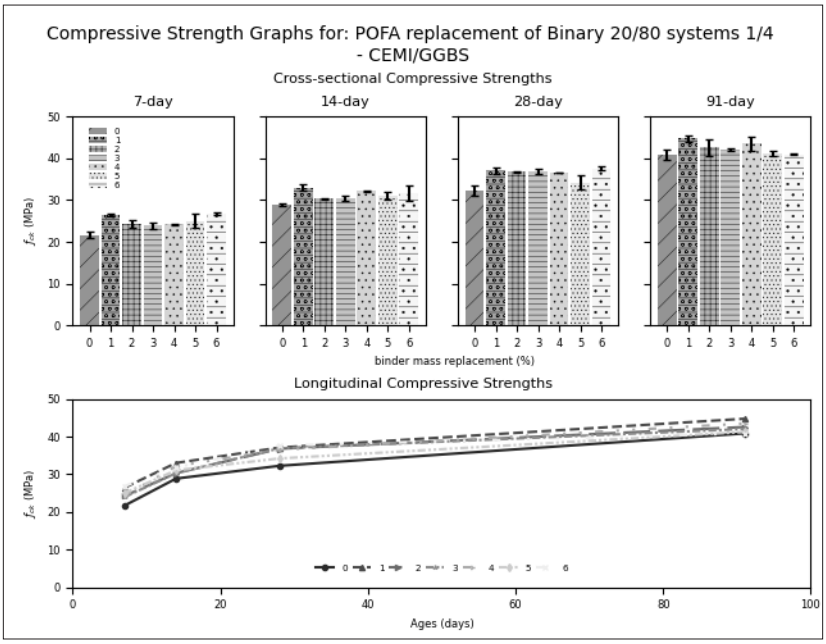

Figure 7: Compressive Strengths of Concrete with POFA Replacement in Binary 20/80 Systems - CEMI/GGBS

Figure 7 indicate that all POFA-containing mixes surpass control strength by 7-days with 1% and 2% replacement remaining equally offset thereafter and higher percentage replacements strength gains beyond 28-days slowing compared to the control. This would indicate that the primary function is not that of latent pozzolanic reaction but more early activation.

While the early-age strength gain observed cannot be attributed solely to a conventional filler effect, given that the POFA particles are generally coarser than the materials they replace, it is possible that their size distribution partially compensates for deficiencies in the overall PSD, contributing indirectly to packing density. Nevertheless, the primary contribution is more likely associated with the dilution effect of K_2O and KCl and the interaction of these highly reactive compounds with the hydration kinetics, resulting in a slight acceleration of early strength development when POFA replaces the composite cement.

Portland-Limestone Cement and Ground Granulated Blast Furnace Slag

Contrary to the CEMI/GGBS system, the CEMII/GGBS system showed a significant decrease in strength at all replacement values past the initial 7-days of curing, where very minor gains had been made by some of the POFA replacement samples over the control, Figure 8.

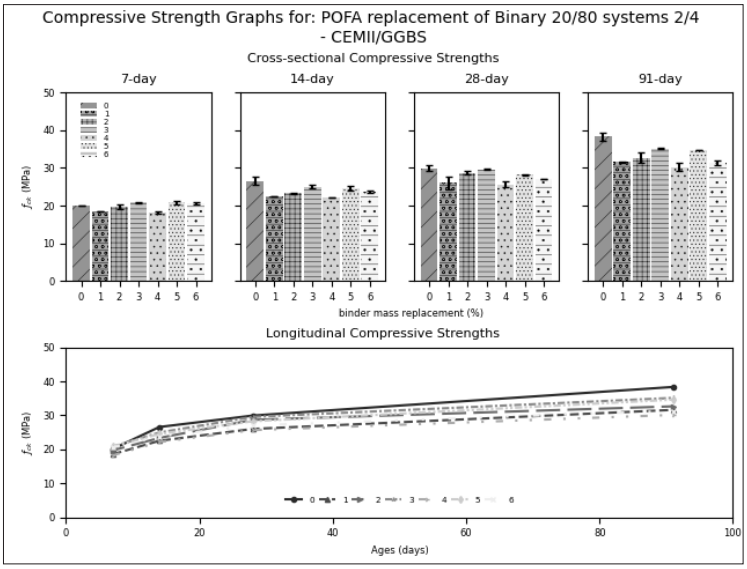

Figure 8: Compressive Strengths of Concrete with POFA Replacement in Binary 20/80 Systems - CEMII/GGBS

Not only is the early age strength affected but the strength progression of the POFA containing samples is slowed.

It is speculated that the increased availability of $CaCO_3$ is interacting with the available K_2O and KCl from the POFA produce other AFM phases during hydration such as the layered double hydroxide of Kuzel's Salt, reducing the amount of C-S-H and C-A-S-H produced.

Hydrated Lime and Ground Granulated Blast Furnace Slag

The CL90/GGBS system differs from both the cement combinations in that the lower POFA replacements are detrimental with improvement in strength gains seen at higher replacement values above 3%, Figure 9, rather than all being either better or inferior than the controls as in CEMI/GGBS or CEMII/GGBS systems, respectively.

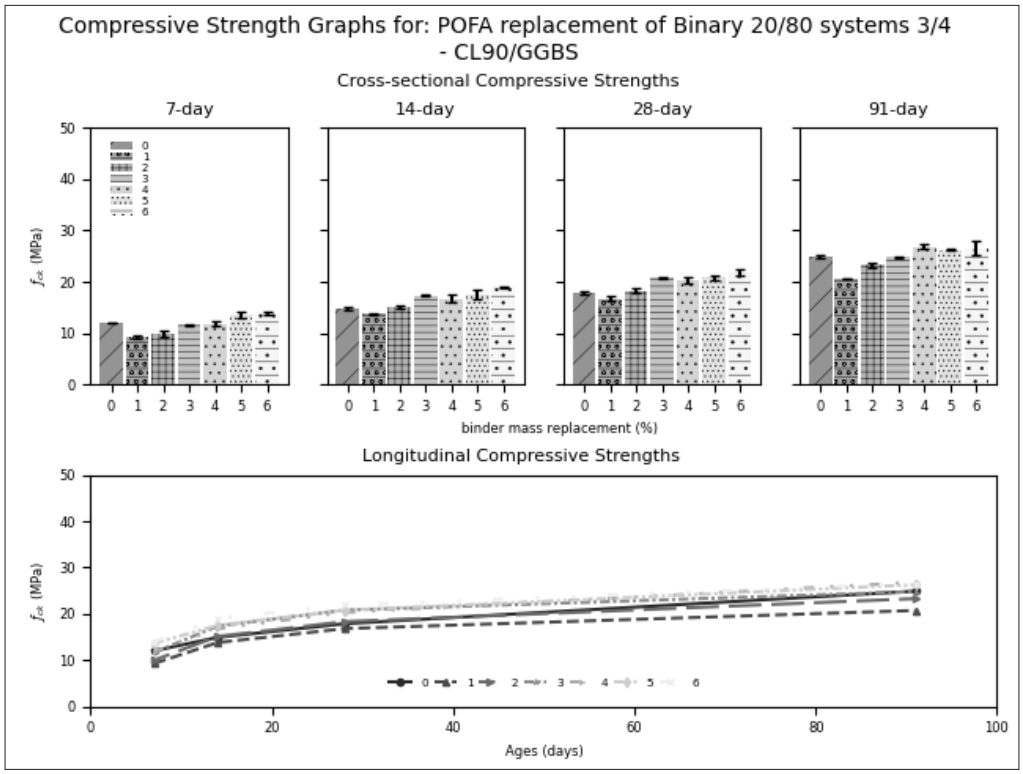

Figure 9: Compressive Strengths of Concrete with POFA Replacement in Binary 20/80 Systems - CL90/GGBS

Low POFA additions (1-2% replacement by binder mass) reduce compressive strength relative to the CL90/GGBS control at early and late ages, with the smallest deficit observed near 28 days. In contrast, higher POFA substitutions (3-6%) produce strengths that are equal to or exceed the control at early ages and show the largest positive differences at 14 and 28 days; by 91 days the rate of additional strength gain in these higher-replacement mixes slows relative to the control, narrowing the long-term margin.

Compressive strength data for 0-6% POFA in CL90/GGBS indicate that 1-2% POFA mixes underperform the control at 7 days and remain below or marginally below the control at 91 days, whereas 3-6% mixes achieve early parity or advantage and peak improvements at 14-28 days. The higher-replacement mixes continue to outperform the low-replacement mixes at 91 days, but the relative advantage decreases over time as the control's latent hydration proceeds.

This atypical response suggests a balance among dilution of hydraulic phases, POFA's filler effect, and the reaction kinetics of CL90/GGBS that depends strongly on replacement level.

At 1-2% POFA the additive appears too small to contribute meaningful packing or pozzolanic benefits and instead produces an effective dilution of hydraulic material, depressing strength. At 3-6% POFA the filler and pozzolanic effects and possible synergistic interaction with GGBS activation become sufficient to offset dilution, yielding equal or improved early- and mid-term strengths.

The reduced incremental gain by 91 days implies either that the control's ongoing hydration and latent reactivity of CL90/GGBS outpace further POFA contributions or that POFA-driven reactions largely complete by 28 days.

Mechanistically plausible factors include replacement-dependent changes in particle packing, altered nucleation behaviour for C-S-H, and shifts in portlandite availability for pozzolanic reaction when CL90 is present. The chemical and mineralogical characteristics of CL90 likely modify how POFA interacts with and activates GGBS relative to CEM I or CEM II, accounting for the distinct temporal pattern observed.

Natural Hydraulic Lime and Ground Granulated Blast Furnace Slag

The pattern of NHL5/GGBS replaced systems' compressive strength gain is similar to CEMII/GGBS systems, albeit at a significant reduction of strength. Whereby, the strengths of the POFA replacement initially indicate a benefit at 3% mass replacement at 7 days. However, being quickly parred by the control and further being outperformed by the control beyond 14

days, significantly and increasing post 28-days.

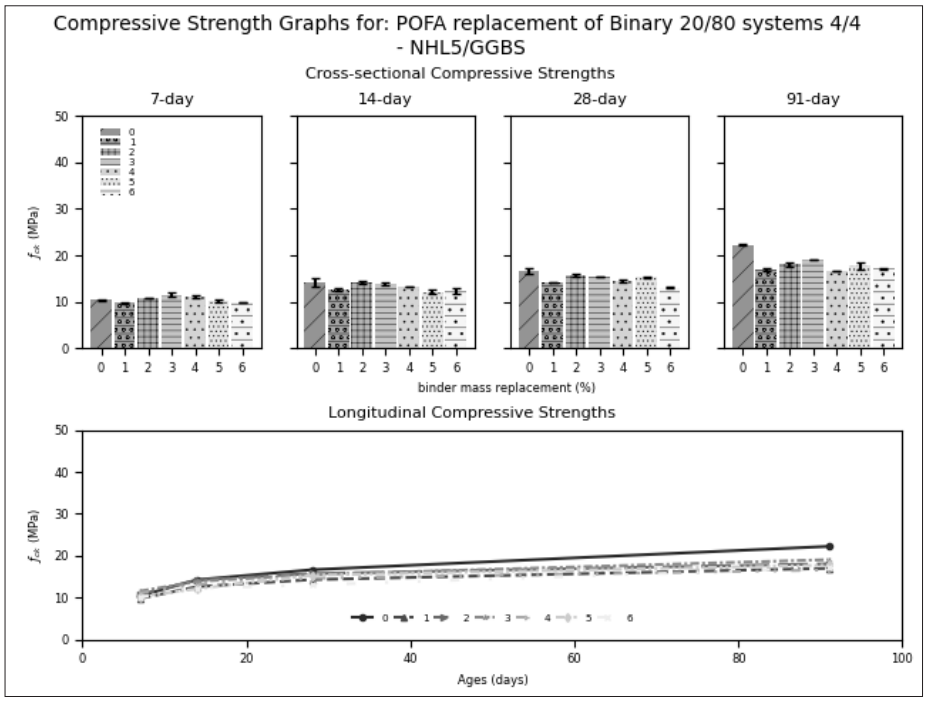

Figure 10: Compressive Strengths of Concrete with POFA Replacement in Binary 20/80 Systems - NHL5/GGBS

The similar behaviour between NHL5/GGBS and CEM II/GGBS systems is consistent with the presence of carbonate species in both binders, which influence early hydration and binder-blending reactions. The transient 3% POFA advantage likely reflects an early filler and nucleation effect that accelerates initial C-S-H formation. The subsequent loss of advantage indicates that the POFA fraction and its reactivity are insufficient to sustain additional long-term binder development against the continuing hydration and latent reactivity of NHL5/GGBS. The reduced absolute strengths observed for NHL5/GGBS relative to CEM II/GGBS reflect the lower intrinsic hydraulicity of NHL5 and its different chemistry, which limit the magnitude of strength gains achievable by adding low levels of POFA.

Flexural Strengths

Three-point flexural strength testing [88], was performed on the 28-day ambient cured prism samples. The highest flexural strengths obtained were from those of the controls of 100% CEMI samples at 4.7MPa followed by the 100% CEMII samples at 3.5MPa. All binary GGBS systems both with and without POFA additions obtained lower flexural strengths, Figure 11.

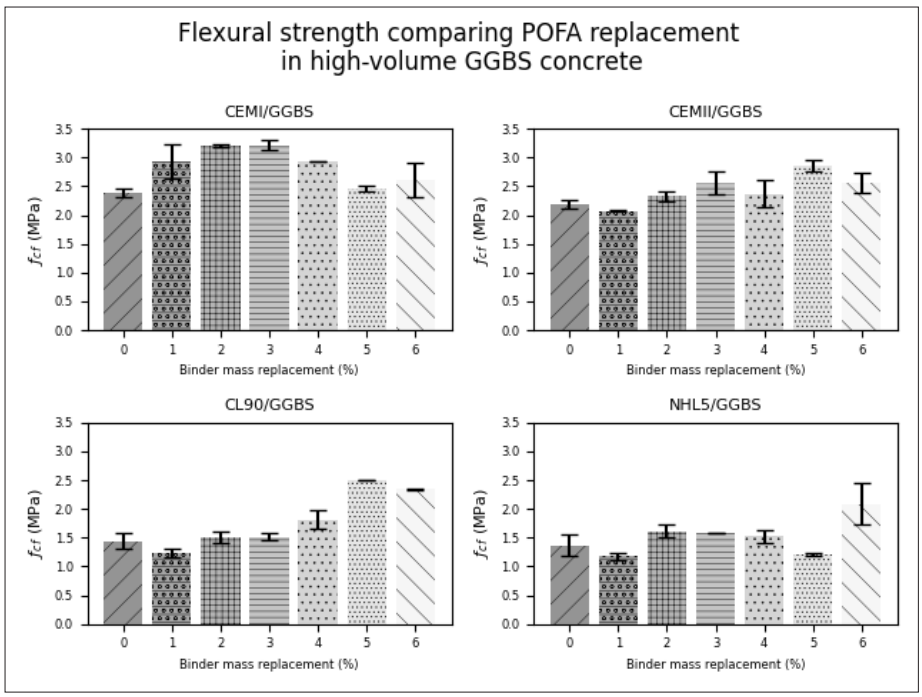

Figure 11: Flexural Strength Comparison - POFA Replacement of Secondary Binders in High-Volume GGBS Concrete at 0.4w/b

In contrast, all binary GGBS systems, both with and without POFA, exhibited lower absolute flexural strengths than their respective pure cement controls. This reduction is likely due to the slower pozzolanic and latent hydraulic reactivity of GGBS, which delays the development of a dense C-S-H matrix at early curing ages.

Nevertheless, the incorporation of POFA into these binary systems consistently enhanced flexural strength relative to the corresponding GGBS-only blends. This improvement suggests that POFA contributes beneficially through a combination of filler effects, improved particle packing, and secondary pozzolanic reactions, which may accelerate the consumption of portlandite and promote the formation of additional C-S-H and other strength-contributing phases.

The optimal POFA content for peak flexural strength varied according to the secondary binder system. For GGBS/CEMI blends, the maximum strength was achieved at 2-3% POFA replacement, indicating that only a modest addition is required to enhance the microstructure without excessively diluting the clinker content.

In the GGBS/CEMII and GGBS/CL90 systems, the peak occurred at 5% POFA, suggesting a greater tolerance for clinker replacement in these matrices, possibly due to synergistic interactions between POFA and the more heterogeneous hydration products of CEMII and hydrated lime.

The GGBS/NHL5 system exhibited a sporadic increase in strength up to 6% POFA, however the large variability in the 6% value and limited trend gives little confidence, necessitating further investigation to explicate further meaning.

Overall, these results indicate that while high-volume GGBS systems cannot match the absolute flexural strength of pure Portland cements at 28 days, targeted incorporation of POFA can partially mitigate this deficiency.

The binder-specific nature of the optimal POFA content underscores the importance of tailoring mix designs to the chemical and physical characteristics of the constituent binders. This finding has practical implications for the development of more sustainable cementitious systems, as it demonstrates that small, optimised additions of agricultural waste-derived pozzolans can enhance performance while contributing to clinker reduction and associated CO_2e.

Curing Regime Comparison

Curing plays a pivotal role in the development of concrete's microstructure, directly influencing its mechanical performance, durability, and long-term serviceability. The hydration of cementitious binders is a moisture- and temperature-dependent process; inadequate curing can result in incomplete hydration, increased porosity, and reduced resistance to environmental degradation. This is particularly critical in systems incorporating high volumes of SCMs, such as GGBS and POFA, where the pozzolanic and latent hydraulic reactions can proceed more slowly than in clinker-rich binders.

The choice of curing regime is therefore a decisive factor in realising the potential benefits of such sustainable binder systems. Water submersion provides a continuous supply of moisture, promoting extended hydration and pozzolanic activity, while ambient curing more closely reflects in-situ conditions where moisture availability may be limited and carbonation can take place. Comparing these regimes offers valuable insight into the sensitivity of high-volume GGBS-POFA concretes to curing conditions, and their capacity to achieve adequate strength and durability under practical construction scenarios.

In this study, the influence of two distinct curing environments, continuous water submersion and ambient exposure, was evaluated at 28 and 91 days. This comparison enables assessment of both early and later-age performance, highlighting the extent to which curing conditions can mitigate or exacerbate the slower strength development typically associated with high-SCM systems. The findings provide a basis for optimising curing practices for sustainable concrete mixtures, ensuring that environmental benefits are not achieved at the expense of structural performance.

Ordinary Portland Cement and Ground Granulated Blast Furnace Slag

The CEMI/GGBS system exhibited markedly greater strength development under water submersion compared to ambient curing at 28 days, up to a POFA replacement level of 4%, beyond which the strengths of the two curing regimes were analogous, Figure 12. By 91 days, all POFA replacement levels demonstrated higher strengths under water curing than under ambient conditions.

Furthermore, all POFA-containing mixes, across both curing regimes, achieved higher strengths than their respective controls, with the sole exception of the 91-day water-cured mix containing 6% POFA, which matched the control strength

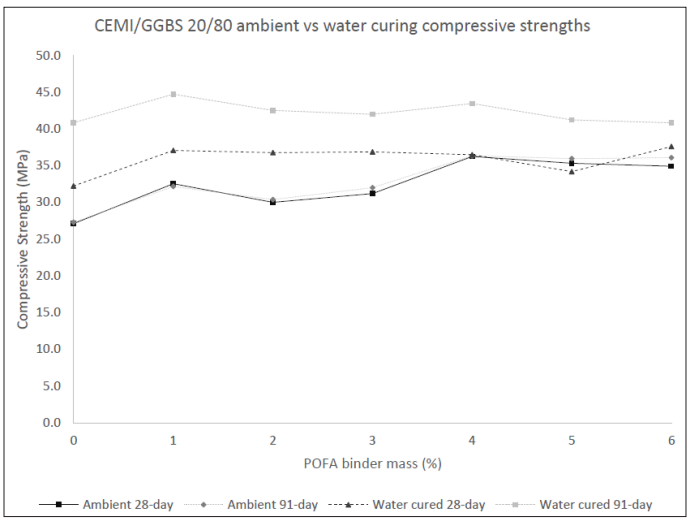

Figure 12: Comparing Curing Regimes for CEMI/GGBS POFA Replacement

Minimal strength development was observed between 28 and 91 days under ambient curing for all POFA replacement levels and the control mix, indicating that carbonation-related strength gain was largely completed within the initial 28 days.

In contrast, specimens cured under continuous water submersion exhibited substantial ongoing strength development beyond 28 days. However, the magnitude of these water-curing gains diminished progressively with increasing POFA content. This trend may suggest that POFA particles interact with, or adsorb, water preferentially during early hydration, thereby reducing the availability of free water for the hydraulic reactions of cement and/or GGBS.

The highest compressive strength for the binder system, 45MPa, was during submerged curing, and for both 28- and 91-day samples the maximum strength occurred at a 1% POFA replacement value. Whereas the maximum achieved compressive strength for the ambient cured samples occurred at a POFA replacement value of 4%.

Portland-Limestone Cement and Ground Granulated Blast Furnace Slag

Similar to the CEMI/GGBS system, the CEMII/GGBS blends exhibited a progressive reduction in the difference between compressive strengths under the two curing regimes as POFA replacement increased. At 6% POFA replacement, the strengths of the ambient- and water-cured specimens were nearly identical, Figure 13. Following an initial reduction in strength at 1% POFA replacement, the ambient-cured specimens demonstrated a gradual increase in compressive strength with further POFA additions. In contrast, the water-cured specimens displayed a general downward trend in strength as POFA content increased.

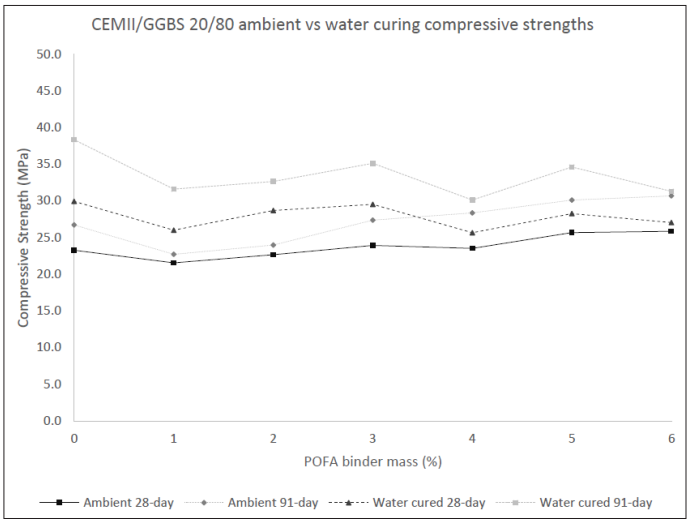

Figure 13: Comparing Curing Regimes for CEMII/GGBS POFA Replacement

At lower replacement levels, ambient-cured specimens showed minimal strength gain between 28 and 91 days; however, strength development improved noticeably for POFA contents above 3%. Conversely, water-submerged specimens exhibited consistent strength gains over the same period across all replacement levels. The highest compressive strength recorded for the CEMII/GGBS system was that of the water-cured control mix at 38 MPa, only marginally lower than the corresponding control in the CEMI/GGBS system.

When considered together, the CEMI/GGBS and CEMII/GGBS systems reveal both commonalities and distinct differences in their response to POFA incorporation and curing regime. In both systems, increasing POFA content progressively reduced the disparity in compressive strength between water- and ambient-cured specimens, with near parity achieved at the highest replacement levels. This convergence suggests that at elevated POFA dosages, the influence of curing environment becomes less pronounced, potentially due to the dominant role of POFA-driven microstructural changes over binder-specific hydration kinetics. However, the direction of strength trends differed between the two systems: in CEMI/GGBS blends, water curing generally enhanced strength across the POFA range, whereas in CEMII/GGBS blends, water-cured specimens exhibited a gradual decline in strength with increasing POFA content. Ambient-cured CEMII/GGBS mixes, in contrast, benefited from higher POFA levels, showing late-age strength gains not observed in the CEMI/GGBS system. These differences may be attributed to the higher limestone content of CEMII, which can influence both the hydration products and the interaction between POFA and the binder matrix, particularly under moisturelimited conditions. Overall, the comparison underscores that while both systems respond positively to optimised POFA incorporation, the optimal dosage and curing strategy are binder-specific, reflecting the complex interplay between clinker chemistry, SCM reactivity, and curing environment.

Hydrated Lime and Ground Granulated Blast Furnace Slag

The CL90/GGBS system followed the general trend observed in other binder configurations, with water-cured specimens consistently outperforming those cured under ambient conditions across all POFA replacement levels. Notably, the 28-day water-cured strengths were broadly comparable to the 91-day ambient-cured strengths, Figure 14, indicating that continuous moisture availability accelerates strength development in this lime-based system.

Following an initial reduction in compressive strength at 1% POFA replacement, both curing regimes exhibited a steady upward trend with increasing POFA content, achieving parity with the control mix at 3% replacement. The highest strength recorded in this series was for the 91-day water-cured specimen containing 4% POFA, with peak strengths for all ages and curing conditions occurring within the 3-5% replacement range. This suggests an optimal dosage window in which POFA contributes positively to microstructural refinement and strength gain without excessively diluting the reactive lime and slag phases.

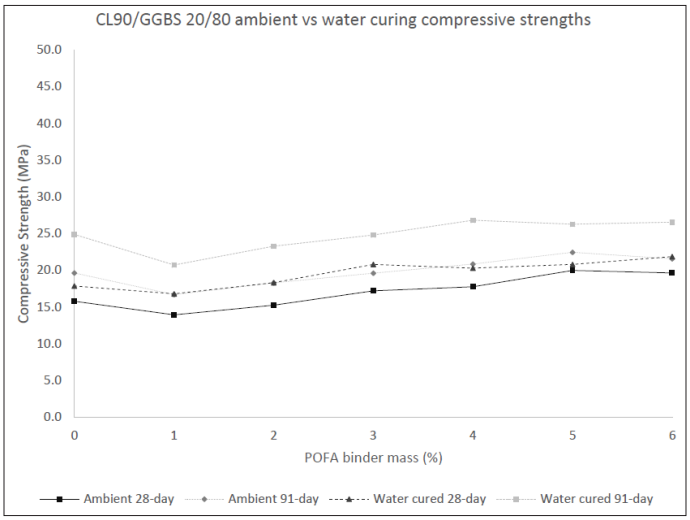

Figure 14: Comparing Curing Regimes for CL90/GGBS POFA Replacement

Unlike the cement-based systems (CEMI/GGBS and CEMII/GGBS), the CL90/GGBS blends did not exhibit a pronounced convergence in strength between the two curing regimes at higher POFA contents. This divergence may be attributed to the fundamentally different hydration and carbonation mechanisms in lime-rich matrices. In the CL90/GGBS system, strength development under ambient conditions is likely dominated by carbonation of calcium hydroxide, a process that is inherently slower and more dependent on CO_2 ingress than the hydration

reactions prevalent in cement systems. Under water curing, however, the availability of moisture promotes continued slag activation with POFA, leading to sustained strength gains over time.

Overall, the CL90/GGBS system demonstrates that POFA can be effectively utilised in lime-based binary binders to enhance mechanical performance, provided that curing conditions are carefully controlled and replacement levels are optimised. The absence of curing regime convergence highlights the importance of moisture availability in maximising the reactivity of both GGBS and POFA in non-cementitious matrices.

Natural Hydraulic Lime and Ground Granulated Blast Furnace Slag

The NHL5/GGBS system exhibited only marginal differences in compressive strength between ambient- and water-cured specimens across all POFA replacement levels, curing ages, and conditions, particularly when compared with the other binder systems investigated. Despite this narrow performance gap, the general trend of water curing producing slightly higher strengths than ambient curing remained evident, Figure 15.

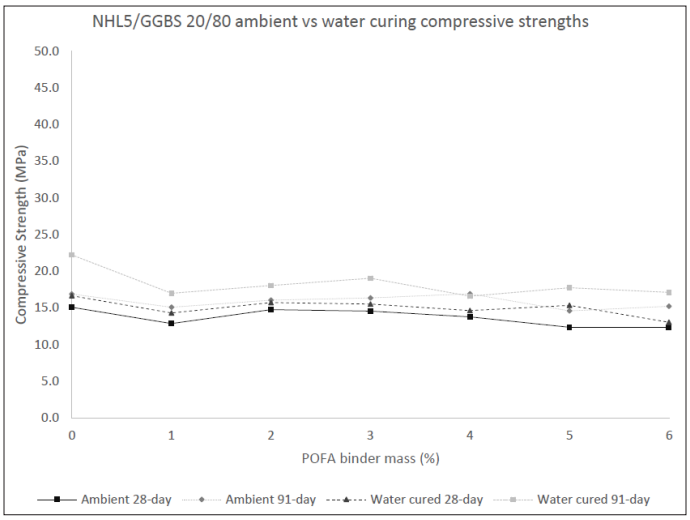

Figure 15: Comparing Curing Regimes for NHL5/GGBS POFA Replacement

As with the CL90/GGBS system, the 28-day water-cured specimens achieved strengths comparable to those of the 91-day ambient-cured specimens, and an initial reduction in compressive strength was observed at 1% POFA replacement. However, in contrast to CL90/GGBS, subsequent increases in POFA content produced only minor variations in strength, with a small, localised peak at approximately 2-3% replacement, followed by a gradual decline at higher dosages. The highest compressive strengths for all curing ages and conditions were recorded for the control mixes, indicating that POFA incorporation did not enhance performance in this high-GGBS/NHL5 configuration.

The limited sensitivity of the NHL5/GGBS system to POFA content and curing regime may be attributed to the inherently slow reactivity of NHL5 and its reliance on carbonation as a primary strength-developing mechanism. In such lime-rich systems, the rate of strength gain is governed more by CO_2 ingress than by moisture availability, which may explain the relatively small performance differential between curing environments. Furthermore, the high GGBS content, while capable of contributing to long-term strength through latent hydraulic reactions, may require more aggressive activation conditions than those provided by NHL5 alone. The introduction of POFA, although potentially beneficial in systems with higher clinker or more reactive lime content, may not significantly influence hydration or carbonation kinetics in this particular binder ratio.

These findings suggest that while POFA can be a valuable SCM in certain lime- or cement-based systems, its benefits are highly dependent on the chemical reactivity of the primary binder and the curing environment. For the high-GGBS/NHL5 combination studied here, optimisation of the NHL5to-GGBS ratio, or the inclusion of additional activators, may be necessary before POFA can deliver measurable performance gains. This does not, however, preclude the possibility that POFA could provide performance benefits at alternative NHL5-to-GGBS ratios.

Indexed Secondary Binder Comparisons

The control samples for each of the secondary binders show a range for the benefit of water curing between 10-50% additional compressive strength decreasing with POFA addition to 0-25% by 6% replacement value, Figure 16, showing a smaller influence of the additional pore water or increased influence of carbonation at higher POFA replacement values.

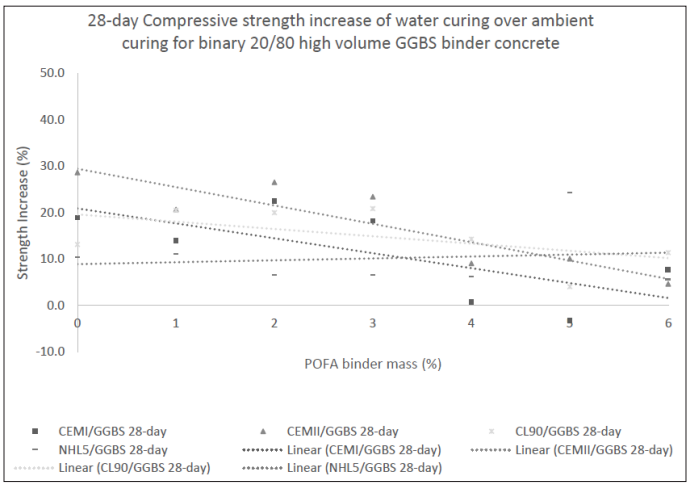

Figure 16: Comparing Secondary Binders Curing Dependencies Indexed to Ambient Conditions

Across all four binder systems, CEMI/GGBS, CEMII/GGBS, CL90/GGBS, and NHL5/GGBS, the general trend of water-cured specimens outperforming ambient-cured specimens was evident, although the magnitude of this advantage varied markedly with binder type and POFA content. In the cement-based systems (CEMI and CEMII), water curing conferred substantial early- and late-age strength benefits, with the performance gap narrowing as POFA replacement increased, reaching near parity at 6% POFA for CEMI/GGBS and CEMII/GGBS. In contrast, the lime-based systems (CL90 and NHL5) exhibited smaller absolute differences between curing regimes, with 28-day water-cured strengths generally matching those of 91-day ambient-cured specimens.

POFA incorporation produced binder-specific responses: CEMI/GGBS and CL90/GGBS showed clear strength optima at 2-3% and 3-5% replacement respectively, CEMII/GGBS peaked at 5%, while NHL5/GGBS displayed only minor variation beyond an initial 1% reduction, with a slight localised peak at 2-3%.

Notably, the highest strengths in the cement systems were achieved by water-cured controls, whereas in the lime-based systems, peak strengths occurred within the mid-range POFA dosages. These findings highlight that the interaction between POFA content,

binder chemistry, and curing regime is highly system-dependent: cement-rich blends benefit most from water curing at low to moderate POFA levels, while lime-rich blends exhibit more modest curing sensitivity but can achieve optimal performance within a narrow POFA range.

The comparative analysis of curing regimes underscores the critical role of moisture availability in unlocking the performance potential of high-volume GGBS-POFA concretes. While continuous water submersion consistently promoted superior strength development, bar a single result, the ability of certain binder-POFA combinations to maintain competitive performance under ambient conditions highlights their practical viability in less controlled environments. These results reinforce the premise that optimised curing strategies, tailored to the specific binder chemistry, can bridge the gap between laboratory performance and field application.

Conclusions and Recommendations

It is evident from the chemical investigations and literature review that the POFA sample is indictive of an unrefined sample that could benefit from further pyro processing and is atypical compared to that generally used for an SCM in concrete.

The key findings from the research are as follows:

- The secondary binder directly contributed to compressive strength development in the order CEMI>CEMII>CL90>NHL5.
- The secondary binder can be directly related to the mechanical properties of the concrete with the order of maximum achieved characteristic water-cured 28-day compressive strength.
- The POFA replacements within each secondary binder had distinct effects, with CEMI and CL90 specimens exhibiting improved mechanical behaviour and CEMII and NHL5 samples exhibiting reduced capacity.
- A similar pattern exists between the compressive strength change dependant on POFA replacement in the CEMII/GGBS and NHL5/GGBS results.
- CL90/GGBS benefits from higher GGBS content, above 80% mass, contrary to the other secondary binders of CEMI, CEMII, and NHL5.
- 3% POFA substitution causes noticeable but manageable early and 28-day strength reductions in both primary OPC and PLC mixes, with proportionally higher loss in PLC.
- All blended binders benefitted from water curing.
- Contrary to the lime blends, the benefit of water curing reduced in the cement blends with increasing POFA.

Chemical and morphological analyses reveal that the POFA sample examined in this study is atypical of conventional SCMs, exhibiting characteristics more akin to industrial by-products such as bypass or flue dust. Its unrefined nature, coupled with unusually high L.O.I and elevated soluble salt content, suggests the need for further pyro-processing and reinforces the importance of rigorous material characterisation during sample preparation, given the compositional variability of POFA across sources. Two distinct morphologies, fine ash and unburnt strands, were identified, warranting fraction-specific chemical and mineralogical analysis to assess their individual reactivity and contributions to binder performance. This study addresses a persistent gap in the literature, where prior research on POFA has often lacked sufficient methodological detail for comparative evaluation. By providing a higher degree of analytical resolution, the study contributes to a more nuanced understanding of POFA's role in low-carbon cementitious systems. Subsequent testing within binary high-volume GGBS binders revealed that GGBS activation was primarily driven by calcium hydroxide, which was disproportionately present in the systems. Given that no separation of activators was undertaken, the potential contribution of potassium-based compounds merits further investigation. Water curing significantly enhanced compressive strength, particularly in cement-based blends, while flexural strength improvements were observed across all systems with targeted POFA additions. However, the chemical composition and mineralogical profile of the POFA used in this study may not directly contribute to secondary pozzolanic activity; instead, observed performance gains are more plausibly attributed to physical mechanisms such as filler effects, improved particle packing, limited latent hydraulic contributions, and early activation effects. Optimal POFA content varied by binder type, ranging from 2-6%, indicating the need for binder-specific optimisation of dosage and curing regimes. For practical implementation, especially in PLC systems, careful control of mix design and curing conditions is essential. Future research should explore advanced activation strategies, longterm performance, and broader material combinations to support the integration of POFA into sustainable binder technologies.

References

1. Olivier JG, Peters JA, Janssens-Maenhout G (2012) Trends in global CO2 emissions. 2012 report. European Commission https://op.europa.eu/en/publication-detail/-/publication/f4b2d6d7-31f4-4ef5-a9df-79a9813311ca/language-en.
2. Quéré C, Andrew RM, Friedlingstein P, Sitch S, Hauck J, et al. (2018) Global carbon budget 2018. Earth System Science Data 10: 2141-2194.
3. Andrew RM (2019) Global CO_2 emissions from cement production, 1928-2018. Earth System Science Data 11: 1675-1710.
4. Scrivener KL, Kirkpatrick RJ (2008) Innovation in use and research on cementitious material. Cement and Concrete Research 38: 128-136.
5. Higgins D, Uren M (1991) The effect of GGBS on the durability of concrete. Concrete 25 https://trid.trb.org/View/376836.
6. Oner A, Akyuz S (2007) An experimental study on optimum usage of GGBS for the compressive strength of concrete. Cement and Concrete Composites 29: 505-514.
7. Thavasumony D, Subash T, Sheeba D (2014) High strength concrete using ground granulated blast furnace slag (GGBS). International Journal of Scientific & Engineering Research 5: 1050-1054.
8. Higgins D (2003) Increased sulfate resistance of GGBS concrete in the presence of carbonate. Cement and Concrete Composites 25: 913-919.
9. Zhao J, Shumuye ED, Wang Z, Bezabih GA (2021) Performance of GGBS cement concrete under natural carbonation and accelerated carbonation exposure. Journal of Engineering 2021: 6659768.
10. Ahmed A, Nadir H, Cunliffe J, Yates C, Yates L, et al.(2021) Potential sustainable cement free limecrete based on GGBS & hydrated lime as an alternative for standardised prescribed concrete applications. Research & Development in Material Science 15: 1753-1763.
11. Karri SK, Rao GR, Raju PM (2015) Strength and durability studies on GGBS concrete. SSRG International Journal of Civil Engineering 2: 34-41.
12. Luo R, Cai Y, Wang C, Huang X (2003) Study of chloride binding and diffusion in GGBS concrete. Cement and Concrete Research 33: 1-7.
13. Pavía S, Condren E (2008) Study of the durability of OPC

versus GGBS concrete on exposure to silage effluent. Journal of Materials in Civil Engineering 20: 313-320.

14. BSI (2011) Cement composition, specifications and conformity criteria for common cements. London, UK: BSI Standards Publication https://www.intertekinform.com/preview/98698894521.pdf?sku=868797_saig_nsai_nsai_2066037&srsltid=AfmBOopsowzgr3chPszzdi1Oi2StAkPz2qMgsPsyi7Z2J1w1B1xLbEj- .
15. Phelipot-Mardelé A, Gabriel S, Christophe L (2015) Super sulfated cement: formulation and uses. Proceedings of the Fifth International Conference on Construction Materials: Performance, Innovations and Structural Implications.
16. Provis JL (2014) Geopolymers and other alkali activated materials: why, how, and what? Materials and Structures 47: 11-25.
17. Arnold W, Astle P, Drewniok M, Forman T, Gibb I, et al.(2023) The efficient use of GGBS in reducing global emissions.
18. Hamada HM, Jokhio GA, Yahaya FM, Humada AM, Gul Y (2018) The present state of the use of palm oil fuel ash (POFA) in concrete. Construction and Building Materials 175: 26-40.
19. Yusuf MO, Johari MAM, Ahmad ZA, Maslehuddin M (2014) Strength and microstructure of alkali-activated binary blended binder containing palm oil fuel ash and ground blastfurnace slag. Construction and Building Materials 52: 504-510.
20. Bamaga S, Ismail MA, Hussin M (2010) Chloride resistance of concrete containing palm oil fuel ash. Cement and Concrete Research 1: 158-166.
21. Awal AA, Shehu I, Ismail M (2015) Effect of cooling regime on the residual performance of high-volume palm oil fuel ash concrete exposed to high temperatures. Construction and Building Materials 98: 875-883.
22. Ahmad M, Omar R, Malek M, Noor NM, Thiruselvam S (2008) Compressive strength of palm oil fuel ash concrete. Proceedings of the International Conference on Construction and Building Technology, Kuala Lumpur, Malaysia https://www.researchgate.net/publication/259935880_Compressive_Strength_of_Palm_Oil_Fuel_Ash_Concrete.
23. Chandara C, Sakai E, Azizli KAM, Ahmad ZA, Hashim SFS (2010) The effect of unburned carbon in palm oil fuel ash on fluidity of cement pastes containing superplasticizer. Construction and Building Materials 24: 1590-1593.
24. Awal ASM, Hussin MW (1999) Durability of high performance concrete containing palm oil fuel ash. In: Lacasse MA and Vanier DJ (eds) Durability of Building Materials and Components 8. Canada: National Research Council Canada 465-474.
25. Pone J, Ahmed A, Hyndman F (2018) Palm oil fuel ash as a cement replacement in concrete. Modern Approaches on Material Science 1(1).
26. Ebienfa P, Yabefa B (Year) The influence of palm oil fuel ash (POFA) on the mechanical properties of Portland limestone cement concrete.
27. Brown OR (2014) Potential of kaolin-palm oil fuel ash mixture as sustainable landfill liner material. Universiti Teknologi Malaysia, Skudai, Malaysia.
28. Islam A, Alengaram UJ, Jumaat MZ, Bashar II (2014) The development of compressive strength of ground granulated blast furnace slag-palm oil fuel ash-fly ash based geopolymer mortar. Materials & Design 56: 833-841.
29. Islam A, Alengaram UJ, Jumaat MZ, Bashar II, Kabir SA (2015) Engineering properties and carbon footprint of ground granulated blast-furnace slag-palm oil fuel ash-based structural geopolymer concrete. Construction and Building Materials 101: 503-521.
30. Yusuf MO, Johari MAM, Ahmad ZA, Maslehuddin M (2014) Evolution of alkaline activated ground blast furnace slag-ultrafine palm oil fuel ash based concrete. Materials & Design 55: 387-393.
31. Abdulaziz Al-Shalif AF (2020) Sequestration of carbon dioxide (CO_2) using bio-foamed concrete brick incorporating Bacillus tequilensis bacteria. Universiti Tun Hussein Onn Malaysia.
32. Abdullah F (2020) A systematic review on bio-sequestration of carbon dioxide in bio-concrete systems: a future direction.
33. Aprianti E (2017) A huge number of artificial waste material can be supplementary cementitious material (SCM) for concrete production - a review part II. Journal of Cleaner Production 142: 4178-4194.
34. Aprianti E (2017) Effect of curing condition on the characteristics of mortar containing high volume supplementary cementitious materials. University of Malaya, Malaysia.
35. Balagosa J, Navea IJ, Lee MJ, Choo YW, Kim H-S, Kim J-M (2024) Dynamic property growth of weathered granite soils stabilized with wood pellet fly ash based binders. Soil Dynamics and Earthquake Engineering 180: 108627.
36. Caneda-Martínez L, Frías M, Sánchez J, Rebolledo N, Flores E, Medina C (2022) Durability of eco-efficient binary cement mortars based on ichu ash: effect on carbonation and chloride resistance. Cement and Concrete Composites 131: 104608.
37. Česnauskas V (2018) Biomass fly ash additive for Portland cement and slag cement. Kauno Technologijos Universitetas https://en.ktu.edu/events/594495/.
38. Duarte LG (2022) Evaluation of the pozzolanic activity of agro-industrial residues in lime suspensions: residue.
39. Hassan DA, Fahmy EH, Shaheen YB, Abou Zeid MN (2012) Use of industrial waste materials for producing mortar and concrete mixes. Proceedings of the Annual Conference Canadian Society for Civil Engineering.
40. Chee HL (2013) Effect of curing regimes on mortar incorporating metakaolin and slag at low water/binder ratio. Malaysia http://eprints.utar.edu.my/850/1/CI%2D2013%2D0907046%2D01.pdf.
41. Hren M, Bosiljkov VB, Legat A (2021) Effects of blended cements and carbonation on chloride-induced corrosion propagation. Cement and Concrete Research 145: 106458.
42. Huseien GF, Memon RP, Baghban MH, Faridmehr I, Wong LS (2024) Effective microorganism solution-imbued sustainable self-curing concrete: evaluation of sorptivity, drying shrinkage and expansion. Case Studies in Construction Materials 20: e03255.
43. Ikeh H (2023) The mechanical properties of wood-doped geopolymer. Forestry and Technology https://erepo.uef.fi/server/api/core/bitstreams/885e4c53-77d5-4d63-a4b9-d89a131f40ea/content.
44. Kemp R, Barteková E, Türkeli S (2017) The innovation trajectory of eco-cement in the Netherlands: a co-evolution analysis. International Economics and Economic Policy 14: 409-429.
45. Kumar EM, Perumal P, Ramamurthy K (2022) Alkali-activated aerated blends: interaction effect of slag with low and high calcium fly ash. Journal of Material Cycles and Waste Management 24: 1378-1395.
46. Mahmud MB (2021) Effect of ceramic waste on geotechnical properties of cement stabilized clay soil 10: 109-120.
47. Martinez CM, Del Bosque IS, Medina G, Frías M, De Rojas MS (2022) Fillers and additions from industrial waste for recycled aggregate concrete. The Structural Integrity of Recycled Aggregate Concrete Produced with Fillers and Pozzolans 105-143.

48. Mishra J, Das SK, Singh SK, Mustakim SM (2019) Development of geopolymer concrete for the protection of environment: a greener alternative to cement. International Journal of Civil Engineering 6: 41-47.
49. Ngui F, Muhammed N, Mutunga FM, Marangu J, Kinoti IK (2022) A review on selected durability parameters on performance of geopolymers containing industrial by-products, agro-wastes and natural pozzolan. Journal of Sustainable Construction Materials and Technologies 7: 375-400.
50. Raghav M, Park T, Yang H-M, Lee S-Y, Karthick S, et al.(2021) Review of the effects of supplementary cementitious materials and chemical additives on the physical, mechanical and durability properties of hydraulic concrete. Materials 14: 7270.
51. Rahman R, Fazlizan A, Asim N, Thongtha A (2021) A review on the utilization of waste material for autoclaved aerated concrete production. Journal of Renewable Materials 9: 61-72.
52. Şahin O (2022) Assessment of the long-term photocatalytic performance of cementitious systems incorporating different mineral admixtures. Construction and Building Materials 354: 129215.
53. Shah V, Scrivener K, Bhattacharjee B, Bishnoi S (2018) Changes in microstructure characteristics of cement paste on carbonation. Cement and Concrete Research 109: 184-197.
54. Sharma R, Khan RA (2016) Effect of different supplementary cementitious materials on mechanical and durability properties of concrete. Journal of Materials and Engineering Structures 3: 129-147.
55. Singh A, Bhadauria SS, Mudgal M, Kushwah SS (2020) Sustainable utilization of industrial by-products for developing cement free concrete: a review. Journal of Engineering https://www.uitrgpv.ac.in/aboutdepartment/frm_viewfacultyprofile.aspx?Staff_id=22833.
56. Suna X, Waia OW, Xiea J, Lia X, Sun X, et al. (2024) Supporting information: biomineralization to prevent microbially induced corrosion on concrete for sustainable marine infrastructure. Environ Sci Technol 58: 522-533.
57. Szcześniak A, Zychowicz J, Stolarski A (2020) Influence of fly ash additive on the properties of concrete with slag cement. Materials 13: 3265.
58. Tahwia AM, Elgendy GM, Amin M (2022) Effect of environmentally friendly materials on steel corrosion resistance of sustainable UHPC in marine environment. Structural Engineering and Mechanics 82: 133-149.
59. Vafaei D, Ma X, Hassanli R, Duan J, Zhuge Y (2022) Microstructural behaviour and shrinkage properties of high-strength fiber-reinforced seawater sea-sand concrete. Construction and Building Materials 320: 126222.
60. Wang S (2015) Cofired biomass fly ashes in mortar: reduction of alkali silica reaction (ASR) expansion, pore solution chemistry and the effects on compressive strength. Construction and Building Materials 82: 123-132.
61. Xie T, Yang G, Zhao X, Xu J, Fang C (2020) A unified model for predicting the compressive strength of recycled aggregate concrete containing supplementary cementitious materials. Journal of Cleaner Production 251: 119752.
62. Younis M, Amin M, Tahwia AM (2022) Durability and mechanical characteristics of sustainable self-curing concrete utilizing crushed ceramic and brick wastes. Case Studies in Construction Materials 17: e01251.
63. Tahwia AM, Elgendy GM, Amin M (2022) Mechanical properties of affordable and sustainable ultra-high-performance concrete. Case Studies in Construction Materials 16: e01069.
64. Zeyad AM, Tayeh BA, Saba AM, Johari M (2018) Workability, setting time and strength of high-strength concrete containing high volume of palm oil fuel ash. The Open Civil Engineering Journal 12: 12.
65. Amran M, Murali G, Fediuk R, Vatin N, Vasilev Y, et al.(2021) Palm oil fuel ash-based eco-efficient concrete: a critical review of the short-term properties. Materials 14: 332.
66. Awal AA, Hussin MW (2011) Effect of palm oil fuel ash in controlling heat of hydration of concrete. Procedia Engineering 14: 2650-2657.
67. Chindaprasirt P, Rukzon S, Sirivivatnanon V (2008) Resistance to chloride penetration of blended Portland cement mortar containing palm oil fuel ash, rice husk ash and fly ash. Construction and Building Materials 22: 932-938.
68. Hussin MW, Ismail MA, Budiea A, Muthusamy K (2009) Durability of high strength concrete containing palm oil fuel ash of different fineness. Malaysian Journal of Civil Engineering 21: 180-194.
69. Bamaga S, Hussin M, Ismail MA (2013) Palm oil fuel ash: promising supplementary cementing materials. KSCE Journal of Civil Engineering 17: 1708-1713.
70. Zarina Y, Al Bakri AM, Kamarudin H, Nizar IK, Rafiza A (2013) Review on the various ash from palm oil waste as geopolymer material. Reviews on Advanced Materials Science 34: 37-43.
71. Alsubari B, Shafigh P, Jumaat MZ, Alengaram UJ (2014) The effect of palm oil fuel ash as a cement replacement material on self-compacting concrete. Applied Mechanics and Materials 567: 529-534.
72. Adnan SH, Wan MH, Jamaluddin N, Zakaria NH (2015) Performance of recycled aggregate containing POFA as additives for cement. Applied Mechanics and Materials 802: 249-254.
73. Hodjati R, Aslani H, Faridmehr I, Awal AA, Kazemi Z (2015) Modification of grout properties in prepacked aggregate concrete incorporating palm oil fuel ash. Indian Journal of Materials Science 2015: 353617.
74. Premalatha P, Vinodh K, Anto L, Nithiya R (2016) Properties of palm ash concrete. International Journal of Engineering Science Invention 5: 29-32.
75. Alnahhal MF, Alengaram UJ, Jumaat MZ, Alqedra MA, Mo KH, et al.(2017) Evaluation of industrial by-products as sustainable pozzolanic materials in recycled aggregate concrete. Sustainability 9: 767.
76. Rajak MA, Majid Z, Ismail M (2019) Pozzolanic activity of nanosized palm oil fuel ash: a comparative assessment with various fineness of palm oil fuel ash. IOP Conference Series: Earth and Environmental Science 220: 012061.
77. Olutoge FA and Kolade AS (2023) Investigation of compressive strength of slag-based geopolymer concrete incorporated with palm oil fuel ash. West Indian Journal of Engineering 45: 77-85.
78. Mo KH, Ling T-C, Alengaram UJ, Yap SP, Yuen CW (2017) Overview of supplementary cementitious materials usage in lightweight aggregate concrete. Construction and Building Materials 139: 403-418.
79. Hamada H, Abed F, Alattar A, Yahaya F, Tayeh B, et al. (2023) Influence of palm oil fuel ash on the high strength and ultra-high-performance concrete: a comprehensive review. Engineering Science and Technology, an International Journal 45: 101492.
80. Al-mulali MZ, Awang H, Khalil HA, Aljoumaily ZS (2015) The incorporation of oil palm ash in concrete as a means of recycling: a review. Cement and Concrete Composites 55:

129-138.

81. Yong Y-K, Lee H-P (2022) Palm oil fly ash (POFA) as a cementitious material in biomass concrete: a feasibility review. Inti Journal 2022 : 8.
82. Joshi A, Craveiro F, Bártolo H (2021) A review on the application of palm oil fuel ash in concrete as a cementitious material for construction. International Conference on Water Energy Food and Sustainability 717-726.
83. Thomas BS, Kumar S, Arel HS (2017) Sustainable concrete containing palm oil fuel ash as a supplementary cementitious material - a review. Renewable and Sustainable Energy Reviews 80: 550-561.
84. Amran M, Lee YH, Fediuk R, Murali G, Mosaberpanah MA, et al.(2021) Palm oil fuel ash-based eco-friendly concrete composite: a critical review of the long-term properties. Materials 14: 7074.
85. BSI (2012) BS EN 933-1:2012 Tests for geometrical properties of aggregates - Part 1: Determination of particle size distribution - Sieving method. British Standards Institution https://www.scribd.com/document/534852953/EN-933-Pt-1-12.
86. BSI (2019) BS EN 12350-2:2019 Testing fresh concrete - Part 2: Slump test. British Standards Institution https://knowledge.bsigroup.com/products/testing-fresh-concrete-slump-test-2.
87. BSI (2019) BS EN 12390-7:2019 Testing hardened concrete - Part 7: Density of hardened concrete. British Standards Institution https://knowledge.bsigroup.com/products/testing-hardened-concrete-density-of-hardened-concrete-2.
88. BSI (2019) BS EN 12390-5:2019 Testing hardened concrete - Part 5: Flexural strength of test specimens. British Standards Institution https://www.scribd.com/document/881367419/BS-EN-12390-5-2019-2021-10-05-05-57-05-PM.
89. BSI (2019) BS EN 12390-3:2019 Testing hardened concrete - Part 3: Compressive strength of test specimens. British Standards Institution https://knowledge.bsigroup.com/products/testing-hardened-concrete-compressive-strength-of-test-specimens-1.
90. BSI (2015) BS EN 459-1:2015 Building lime - Part 1: Definitions, specifications and conformity criteria. British Standards Institution https://knowledge.bsigroup.com/products/building-lime-definitions-specifications-and-conformity-criteria.
91. BSI (2006) BS EN 15167-1:2006 Ground granulated blast furnace slag for use in concrete, mortar and grout - Part 1: Definitions, specifications and conformity criteria. British Standards Institution https://knowledge.bsigroup.com/products/ground-granulated-blast-furnace-slag-for-use-in-concrete-mortar-and-grout-definitions-specifications-and-conformity-criteria.
92. Teji A, Ahmed A, Zhou K, Yates C, Yates L (2025) Sustainable zero-Portland cement limecrete produced from binary ground granulated blast furnace slag and natural hydraulic lime as an alternative to standardised concrete. Journal of Material Sciences & Manufacturing Research 1-16.
93. BSI (2011) BS EN 197-1:2011 Cement - Part 1: Composition, specifications and conformity criteria for common cements. British Standards Institution.
94. BSI (2013) BS EN 12620:2013 Aggregates for concrete. British Standards Institution https://landingpage.bsigroup.com/LandingPage/Undated?UPI=000000000030152181.
95. Dayarathne W, Galappaththi G, Perera K, Nanayakkara S (2013) Evaluation of the potential for delayed ettringite formation in concrete. National Engineering Conference 59-66.
96. Taylor H, Famy C, Scrivener K (2001) Delayed ettringite formation. Cement and Concrete Research 31: 683-693.
97. Pourchet S, Regnaud L, Perez J-P, Nonat A (2009) Early C3A hydration in the presence of different kinds of calcium sulfate. Cement and Concrete Research 39: 989-996.
98. Bullard JW, Jennings HM, Livingston RA, Nonat A, Scherer GW, et al.(2011) Mechanisms of cement hydration. Cement and Concrete Research 41: 1208-1223.
99. Poyet S, Le Bescop P, Pierre M, Chomat L, Blanc C (2012) Accelerated leaching of cementitious materials using ammonium nitrate (6M): influence of test conditions. European Journal of Environmental and Civil Engineering 16: 336-351.
100. Vollpracht A, Lothenbach B, Snellings R, Haufe J (2016) The pore solution of blended cements: a review. Materials and Structures 49: 3341-3367.
101. Fournier B and Bérubé M-A (2000) Alkali-aggregate reaction in concrete: a review of basic concepts and engineering implications. Canadian Journal of Civil Engineering 27: 167-191.
102. Wang D, Cheng P, Xiong W, Song T, Wu Z (2012) Influences of soluble salts on adsorption properties of polycarboxylate superplasticizers. Journal of Wuhan University of Technology - Materials Science Edition 27: 684-688.
103. Sola E, Ožbolt J, Balabanić G, Mir Z (2019) Experimental and numerical study of accelerated corrosion of steel reinforcement in concrete: transport of corrosion products. Cement and Concrete Research 120: 119-131.
104. Tuutti K (1982) Corrosion of steel in concrete. KTH Royal Institute of Technology https://portal.research.lu.se/en/publications/corrosion-of-steel-in-concrete/
105. Angst U, Elsener B, Larsen CK, Vennesland Ø (2009) Critical chloride content in reinforced concrete - a review. Cement and Concrete Research 39: 1122-1138.
106. Hausmann DA (1967) Steel corrosion in concrete - how does it occur?. Materials Protection 6: 19-23.
107. BSI (2023) BS 8500-1:2023 Concrete - Complementary British Standard to BS EN 206 - Part 1: Method of specifying and guidance for the specifier. British Standards Institution.
108. Xu P, Jiang L, Guo M-Z, Zha J, Chen L, et al. (2019) Influence of sulfate salt type on passive film of steel in simulated concrete pore solution. Construction and Building Materials 223: 352-359.
109. Ukpata JO, Ogirigbo OR, Black L (2022) Resistance of concretes to external chlorides in the presence and absence of sulphates: a review. Applied Sciences 13: 182.
110. Wang ZP, Chen YT, Peng X, Xu LL (2021) Different chlorides attack on the hydration of calcium aluminate cement at 5-40 °C. Materials Science Forum 247-254.
111. Sanytsky M, Kropyvnytska T, Shyiko O (2023) Effect of potassium sulfate on the Portland cement pastes setting behavior. Chemistry & Chemical Technology 17: 170-178.
112. Liang K, Cui K, Sabri MMS, Huang J (2022) Influence factors in the wide application of alkali-activated materials: a critical review about efflorescence. Materials 15: 6436.
113. Czapik P, Zapała-Sławeta J, Owsiak Z, Stępień P (2020) Hydration of cement by-pass dust. Construction and Building Materials 231: 117139.
114. Vassilev SV, Baxter D, Andersen LK, Vassileva CG (2013) An overview of the composition and application of biomass ash. Part 1: phase-mineral and chemical composition and classification. Fuel 105: 40-76.
115. Mesbah A, François M, Cau-dit-Coumes C, Frizon F, Filinchuk Y, Leroux F, et al.(2011) Crystal structure of Kuzel's salt 3CaO·Al2O3·1/2CaSO4·1/2CaCl2·11H2O determined

by synchrotron powder diffraction. Cement and Concrete Research 41: 504-509.

116. Amini IN, Ekaputri JJ (2022) The effect of GGBFS and additional cement, water and superplasticizer on the mechanical properties of workable geopolymer concrete. Green Materials and Electronic Packaging Interconnect Technology Symposium 387-401.

117. Wilson W, Gonthier JN, Georget F and Scrivener KL (2022) Insights on chemical and physical chloride binding in blended cement pastes. Cement and Concrete Research 156: 106747.

118. Githachuri KU and Alexander MG (2013) Durability performance potential and strength of blended Portland limestone cement concrete. Cement and Concrete Composites 39: 115-121.